ResearchGate

See discussions, stats, and author profiles for this publication at: https://www.researchgate.net/publication/267335199

Vorticity generation and conservation for two-dimensional interfaces and boundaries

Article *in* Journal of Fluid Mechanics · November 2014
DOI: 10.1017/jfm.2014.520

CITATIONS
13

READS
171

4 authors, including:

Morten Brøns
Technical University of Denmark
94 PUBLICATIONS **1,061** CITATIONS

SEE PROFILE

Mark C. Thompson
Monash University (Australia)
336 PUBLICATIONS **3,837** CITATIONS

SEE PROFILE

Kerry Hourigan
Monash University (Australia)
301 PUBLICATIONS **3,557** CITATIONS

SEE PROFILE

Some of the authors of this publication are also working on these related projects:

Project Aerodynamics of a rotating and flapping insect wing View project

Project Computational Analysis of the Slipstream Characteristics of High-Speed Trains View project

All content following this page was uploaded by Kerry Hourigan on 26 October 2014.

The user has requested enhancement of the downloaded file.

J. Fluid Mech. (2014), *vol.* 758, *pp.* 63–93. © Cambridge University Press 2014
doi:10.1017/jfm.2014.520

Vorticity generation and conservation for two-dimensional interfaces and boundaries

M. Brøns[1], M. C. Thompson[2], T. Leweke[3] and K. Hourigan[2,4,†]

[1]Department of Applied Mathematics and Computer Science, Technical University of Denmark, DK-2800 Lyngby, Denmark

[2]Fluids Laboratory for Aeronautical and Industrial Research (FLAIR), Department of Mechanical and Aerospace Engineering, Monash University, Melbourne, VIC 3800, Australia

[3]IRPHE, UMR 7342, CNRS, Aix-Marseille Université, Centrale Marseille, 13384 Marseille, France

[4]Division of Biological Engineering, Monash University, Melbourne, VIC 3800, Australia

(Received 13 March 2014; revised 4 June 2014; accepted 4 September 2014)

The generation, redistribution and, importantly, conservation of vorticity and circulation is studied for incompressible Newtonian fluids in planar and axisymmetric geometries. A generalised formulation of the vorticity at the interface between two fluids for both no-slip and stress-free conditions is presented. Illustrative examples are provided for planar Couette flow, Poiseuille flow, the spin-up of a circular cylinder, and a cylinder below a free surface. For the last example, it is shown that, although large imbalances between positive and negative vorticity appear in the wake, the balance is found in the vortex sheet representing the stress-free surface.

Key words: general fluid mechanics, vortex flows, vortex interactions

1. Introduction

The original motivation for this article arose from the conundrum presented by the problem of the flow past a submerged circular cylinder (Sheridan, Lin & Rockwell 1997; Reichl, Hourigan & Thompson 2005; Bozkaya *et al.* 2011). As the gap between the cylinder and the free surface decreases, the vorticity strongly shed from the top surface of the cylinder remarkably, and rapidly, disappears in the wake, leaving vorticity of only one sign in the flow (see figure 1). From our conversations within the fluid mechanics community, it appeared that the solution to this puzzle is not trivial. The apparent violation of the conservation of vorticity (or, more precisely, circulation) led us to consider the more general problem of how vorticity is generated and diffused at interfaces, and under what conditions the corresponding circulation is conserved. Even the simpler problem of what happens over time to vorticity when a cylinder in an initially motionless fluid is impulsively spun-up appears, in general, to be not obvious. As noted by Morton (1984), and still the case, the origin, transport, conservation and behaviour near boundaries of vorticity are often poorly understood.

We therefore concluded that it could be valuable to researchers in the community to present a clear and concise formulation of vorticity generation at interfaces, both non-slip and stress-free. This is the subject of the first part of this article. In a second part,

† Email address for correspondence: kerry.hourigan@monash.edu

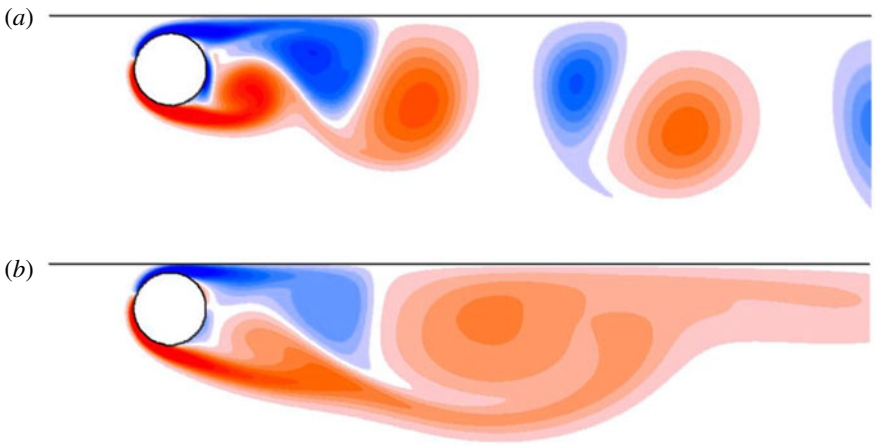

FIGURE 1. (Colour online) Vorticity field for flow past a cylinder submerged beneath a stress-free surface for (*a*) $G/D = 0.25$ and (*b*) $G/D = 0.125$. Each image corresponds to the same time after startup of $t \simeq 24D/U$. The Reynolds number is $Re = 180$ (see § 4 for notation). As the cylinder is placed closer to the free surface, the clockwise vorticity shed from the top of the cylinder appears to vanish as it is advected downstream.

we shall consider a number of instructive examples, including the rotating cylinder, before returning to the particular example of the submerged cylinder. For simplicity, we restrict the discussion to two-dimensional flows.

Vorticity is one of the most important physical quantities in fluid mechanics. Boundary layers, wakes, turbulence and many other phenomena owe their presence to, and are essentially defined by, vorticity and vortices, which are 'the sinews and muscles of fluid motions' (Küchemann 1965). The physics of a given fluid flow is often more effectively illustrated through vorticity than velocity fields. Vorticity, $\boldsymbol{\omega}$, is defined precisely mathematically by

$$\boldsymbol{\omega}(\boldsymbol{r}, t) = \nabla \times \boldsymbol{u}(\boldsymbol{r}, t), \tag{1.1}$$

where $\boldsymbol{u}$ is the local velocity at a point $\boldsymbol{r}$ in space at time t. The vorticity vector represents twice the local average of angular velocity of material lines. In particular, if the fluid is locally in solid-body motion, the axis of rotation is given by the direction of $\boldsymbol{\omega}$, and the angular velocity by $|\boldsymbol{\omega}/2|$.

The generation and redistribution of vorticity in a fluid flow has been discussed by a number of authors, including Longuet-Higgins (1953, 1992, 1998), Lighthill (1963), Batchelor (1967), Morton (1984), Lugt (1987), Ohring & Lugt (1991), Wu (1995), Wu & Wu (1996), Lundgren & Koumoutsakos (1999) and Zhang, Shen & Yue (1999). Rather than specifying a mechanism for its origin, Lighthill (1963) and Batchelor (1967) provide the balance between vorticity generation and its diffusion at a solid wall. Morton (1984) distinguishes between vorticity generation and diffusion, i.e. he separates the accelerations at a solid boundary leading to vorticity generation from its subsequent diffusion away from the boundary. Lundgren & Koumoutsakos (1999) study the appearance and conservation of vorticity in the case of a free-surface boundary. Here, we seek to generalise the description and interpretation to a range of interfaces and boundaries.

In primitive variables (velocity and pressure), the velocity field, and hence the derived vorticity field, is determined through the boundary conditions on the velocity and pressure. Taking the curl of the Navier–Stokes equation eliminates the pressure term. However, as Morton (1984) has pointed out, the resulting Helmholtz vorticity equation for an incompressible fluid with uniform density,

$$\frac{\partial \boldsymbol{\omega}}{\partial t} + (\boldsymbol{u} \cdot \nabla)\boldsymbol{\omega} = (\boldsymbol{\omega} \cdot \nabla)\boldsymbol{u} + \nu \nabla^2 \boldsymbol{\omega}, \tag{1.2}$$

where ν is the kinematic viscosity, is of limited use concerning the issue of vorticity generation, because it contains no true source term. The first term on the right is a processing term describing the local amplification (or concentration) of vorticity by stretching and tilting of vortex filaments. The second term on the right represents viscous diffusion, i.e. the spreading of vorticity due to viscosity. For a homogeneous fluid, vorticity is generated only at boundaries. Batchelor (1967) concluded that the boundary conditions on vorticity are given, in effect, by those on velocity.

Morton (1984) sought a dynamical formulation for the generation of vorticity: he focused on the flow next to a solid wall and concluded that vorticity is generated at boundaries by the relative acceleration of fluid and wall. This vorticity is produced instantaneously, either from the fluid side by tangential pressure gradients, or from the wall side by acceleration of the boundary, and this generation is partially masked by viscous diffusion when there is continuing production. Morton (1984) also found that, for an impulsive change, wall stress does not produce vorticity, and that the only means of decay or loss of circulation is by cross-diffusion and annihilation of vorticity of opposite signs.

Lundgren & Koumoutsakos (1999) examined the case of a free surface and showed that vorticity is conserved. That is, vorticity is not lost through the free surface, but rather is 'stored' in the vortex sheet representing the free surface. This is an important result that has often been debated in the literature, but which also needs to emerge in our present formulation. Furthermore, enforcing the condition of zero shear stress, they found that vorticity 'develops', 'leaks' or 'is generated' at a curved free surface, along which there is a relative flow.

The aim of this article is to provide both a description of the generation of vorticity at two-dimensional interfaces between generalised fluids (ranging from a vacuum to a solid) and for boundary conditions at the interface ranging from stress-free to no-slip, thus generalising the important previous works of Morton (1984) and Lundgren & Koumoutsakos (1999). Furthermore, a number of examples are considered to demonstrate the power of this generalised formulation, and to provide the reader with a physical insight into the generation, redistribution and conservation of vorticity and circulation.

2. Vorticity at the interface of two fluids

2.1. *Generation of vorticity at an interface*

In the present paper we study the two-dimensional flow of two Newtonian incompressible immiscible fluids, divided by an interface, which may be unsteady. Each fluid is assumed to have constant material properties, i.e. constant density and viscosity.

Consider first a single such fluid in some domain in the plane, without boundaries or interfaces. We denote by $\boldsymbol{u}$ the fluid velocity, and ω its vorticity, which is now

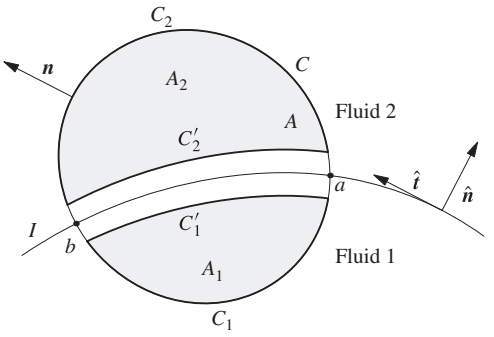

FIGURE 2. The interface I with normal vector $\hat{\boldsymbol{n}}$ and tangential vector $\hat{\boldsymbol{t}}$, forming a right-handed coordinate system. Shaded subregions A_1, A_2 of the region A in each fluid are bounded by the curves C_1, C_1' and C_2, C_2' respectively. The outward normal vector of a region is denoted $\boldsymbol{n}$.

a scalar. Let A be a material region in the domain, bounded by the simple curve C. From Stokes' theorem, the circulation Γ_A contained in A (sometimes also referred to as the 'total vorticity' in A) is equal to the surface integral of the vorticity:

$$\Gamma_A = \oint_C \boldsymbol{u} \cdot \mathrm{d}\boldsymbol{s} = \int_A \omega \, \mathrm{d}A. \tag{2.1}$$

Here, s is the curvilinear distance (arclength) along the contour C, and $\mathrm{d}\boldsymbol{s}$ a (vector) line element of this contour. From a standard application of the divergence theorem on the vorticity transport equation, one obtains for the rate of change of the circulation in A,

$$\frac{\mathrm{d}\Gamma_A}{\mathrm{d}t} = \frac{\mathrm{d}}{\mathrm{d}t} \int_A \omega \, \mathrm{d}A = \oint_C \nu \nabla\omega \cdot \boldsymbol{n} \, \mathrm{d}s, \tag{2.2}$$

where $\boldsymbol{n}$ is the outward normal. Equation (2.2) states that the total vorticity (or circulation) of A changes only because vorticity diffuses across the boundary, the flux into A being given by $\nu\nabla\omega \cdot \boldsymbol{n}$. Thus, there are no sources of vorticity.

Assume now that an interface between two fluids passes through A, as shown in figure 2. We assume that all relevant physical quantities and all of their derivatives have finite limits as the interface is approached in each of the fluids. The limit value of a quantity for an approach in fluid 1 (2) is denoted by the subscript 1 (2). Only when a quantity q is continuous across the interface is it well defined at the interface. Otherwise, only the jump at the interface, defined as

$$[\![q]\!] = q_2 - q_1, \tag{2.3}$$

is single-valued.

Owing to these possible discontinuities, we cannot use the divergence theorem as above directly on A. We may, however, approximate the parts of A in each fluid with subregions A_1 and A_2, as shown in figure 2, and use (2.2) on each subregion. By addition, one obtains

$$\frac{\mathrm{d}}{\mathrm{d}t} \int_{A_1 \cup A_2} \omega \, \mathrm{d}A = \int_{C_1} \nu_1 \nabla\omega \cdot \boldsymbol{n} \, \mathrm{d}s + \int_{C_2} \nu_2 \nabla\omega \cdot \boldsymbol{n} \, \mathrm{d}s + \int_{C_1'} \nu_1 \nabla\omega \cdot \boldsymbol{n} \, \mathrm{d}s + \int_{C_2'} \nu_2 \nabla\omega \cdot \boldsymbol{n} \, \mathrm{d}s. \tag{2.4}$$

The contours C_1, C_2, C_1' and C_2' are defined in figure 2. Let σ_1 denote the vorticity flux at the interface into fluid 1 and likewise σ_2 the vorticity flux out of fluid 2,

$$\sigma_1 = \nu_1 \nabla\omega_1 \cdot \hat{\boldsymbol{n}}, \quad \sigma_2 = \nu_2 \nabla\omega_2 \cdot \hat{\boldsymbol{n}}, \tag{2.5a,b}$$

where $\hat{\boldsymbol{n}}$ is the normal to the surface pointing into fluid 2. Now we let C_1' and C_2' approach the interface I. Then $A_1 \cup A_2 \to A$, and we get from (2.4)

$$\frac{\mathrm{d}}{\mathrm{d}t}\int_A \omega \,\mathrm{d}A = \oint_C \nu \nabla\omega \cdot \boldsymbol{n}\,\mathrm{d}s - \int_a^b [\![\sigma]\!]\,\mathrm{d}s, \tag{2.6}$$

since $\boldsymbol{n} \to \hat{\boldsymbol{n}}$ along C_1' as $C_1' \to I$ and $\boldsymbol{n} \to -\hat{\boldsymbol{n}}$ along C_2' as $C_2' \to I$. In the last integral on the right, s is again the curvilinear coordinate, this time along the interface I. In (2.6), one can think of $[\![\sigma]\!]$ as the density of a source of vorticity located at the interface. However, some care should be taken with this interpretation, since $[\![\sigma]\!]$ only measures the total flux of vorticity out of the interface and into the fluids. It does not say anything about the values of the individual fluxes σ_1 and σ_2 into each fluid. Also, $[\![\sigma]\!]$ is specified in terms of the actual flow, and is in this sense a quantity that can only be found *a posteriori*, after the flow field has been determined otherwise.

Further information about the vorticity source $[\![\sigma]\!]$ can be found from the momentum transport equation. Consider an interior point in the fluid and let $\hat{\boldsymbol{n}}$ and $\hat{\boldsymbol{t}}$ be unit vectors forming a right-handed coordinate system at the given point. It follows by simple computations from the momentum transport equation and the equation of continuity that

$$\frac{\mathrm{d}\boldsymbol{u}}{\mathrm{d}t} \cdot \hat{\boldsymbol{t}} = -\frac{1}{\rho}\nabla p \cdot \hat{\boldsymbol{t}} + \nu \nabla\omega \cdot \hat{\boldsymbol{n}}, \tag{2.7}$$

which links the vorticity flux to the tangential acceleration and the pressure gradient. From kinematical considerations (see appendix A), one finds at the interface in one fluid

$$\frac{\mathrm{d}\boldsymbol{u}}{\mathrm{d}t} \cdot \hat{\boldsymbol{t}} = \frac{\mathrm{d}}{\mathrm{d}t}(\boldsymbol{u} \cdot \hat{\boldsymbol{t}}) + \kappa(\boldsymbol{u} \cdot \hat{\boldsymbol{n}})(\boldsymbol{u} \cdot \hat{\boldsymbol{t}}) - \frac{1}{2}\frac{\partial}{\partial s}(\boldsymbol{u} \cdot \hat{\boldsymbol{n}})^2, \tag{2.8}$$

where

$$\kappa = \frac{\partial \hat{\boldsymbol{n}}}{\partial s} \cdot \hat{\boldsymbol{t}} \tag{2.9}$$

is the curvature of the interface, such that

$$\sigma = \nu \nabla\omega \cdot \hat{\boldsymbol{n}} = \frac{\mathrm{d}}{\mathrm{d}t}(\boldsymbol{u} \cdot \hat{\boldsymbol{t}}) + \frac{1}{\rho}\nabla p \cdot \hat{\boldsymbol{t}} + \kappa(\boldsymbol{u} \cdot \hat{\boldsymbol{n}})(\boldsymbol{u} \cdot \hat{\boldsymbol{t}}) - \frac{1}{2}\frac{\partial}{\partial s}(\boldsymbol{u} \cdot \hat{\boldsymbol{n}})^2. \tag{2.10}$$

This result is also obtained by Lundgren & Koumoutsakos (1999, their equation (23)), except that here we solve for the vorticity flux and do not consider external forces such as gravity. Applying (2.10) at the interface in each fluid, with $\hat{\boldsymbol{n}}$ again being the surface normal vector pointing into fluid 2 and $\hat{\boldsymbol{t}}$ the tangent vector of the interface, and subtracting, we get

$$[\![\sigma]\!] = \frac{\mathrm{d}\gamma}{\mathrm{d}t} + \frac{\partial}{\partial s}\left[\!\!\left[\frac{p}{\rho}\right]\!\!\right] + \kappa\,[\![(\boldsymbol{u} \cdot \hat{\boldsymbol{n}})(\boldsymbol{u} \cdot \hat{\boldsymbol{t}})]\!]\,, \tag{2.11}$$

where

$$\gamma = [\![\boldsymbol{u}\cdot\hat{\boldsymbol{t}}]\!] \tag{2.12}$$

is the strength of the vortex sheet at the interface, which exists if there is a jump in tangential velocity. The jump in the last term on the right of (2.10) is zero, since the normal velocity is single-valued at the interface for continuity.

We emphasise that the vortex sheet that appears at the interface is a consequence of the bookkeeping of the vorticity flux only. It is not the result of a modelling of the vorticity distribution close to the interface. Only the Navier–Stokes equations and continuity of the flow fields in each fluid are assumed and the analysis is completely general, independent of Reynolds number, etc. If, however, the present approach is to be turned into a numerical method, as discussed by Lundgren & Koumoutsakos (1999), some modelling of the vorticity created and stored at the interface must be introduced.

Equation (2.11) illustrates the fundamental mechanisms for generating vorticity at an interface between viscous incompressible Newtonian fluids. The first two terms on the right are those identified by Morton (1984) at a solid wall, but generalised here for any fluid interface. The first term is the relative tangential acceleration between the two fluids at the interface. The second term is the differential tangential pressure (divided by density) gradient in the two fluids at the interface. The third term is non-zero only when the interface is unsteady, with a non-zero normal velocity component ($\boldsymbol{u}\cdot\hat{\boldsymbol{n}}\neq 0$), and curved ($\kappa\neq 0$).

The relative acceleration or differential pressure gradient at an interface either can be generated through the application of external forces or results from internal pressure gradients or accelerations due to viscous shear stresses.

However, in order to generate a net amount of circulation, an external force or torque is required. Internal stresses can result in the appearance of vorticity locally at an interface, but this is accompanied by the appearance of the corresponding circulation of equal magnitude and opposite sign elsewhere. This conservation is demonstrated below.

We conclude this section by discussing the role of surface tension. It appears in the pressure boundary condition, which expresses the continuity of normal stress at the interface. The previous developments were independent of this boundary condition, which is

$$-p_1+\mu_1\,\hat{\boldsymbol{n}}\cdot\boldsymbol{D}_1\cdot\hat{\boldsymbol{n}}+T\kappa=-p_2+\mu_2\,\hat{\boldsymbol{n}}\cdot\boldsymbol{D}_2\cdot\hat{\boldsymbol{n}}, \tag{2.13}$$

where $\mu=\rho\nu$ is the dynamic viscosity, $\boldsymbol{D}$ is the symmetric part of the velocity gradient tensor and T is surface tension. After some algebra (see Lundgren & Koumoutsakos (1999) for details) one finds

$$\hat{\boldsymbol{n}}\cdot\boldsymbol{D}\cdot\hat{\boldsymbol{n}}=-2\frac{\partial}{\partial s}(\boldsymbol{u}\cdot\hat{\boldsymbol{t}})-2\kappa\boldsymbol{u}\cdot\hat{\boldsymbol{n}}, \tag{2.14}$$

such that (2.13) can be written as

$$[\![p]\!]=-2\left[\!\!\left[\mu\frac{\partial}{\partial s}(\boldsymbol{u}\cdot\hat{\boldsymbol{t}})\right]\!\!\right]-T\kappa. \tag{2.15}$$

Here we have used that $[\![\boldsymbol{u}\cdot\hat{\boldsymbol{n}}]\!]=0$. Since

$$\left[\!\!\left[\frac{p}{\rho}\right]\!\!\right]=\frac{1}{\rho_2}[\![p]\!]+\left[\!\!\left[\frac{1}{\rho}\right]\!\!\right]p_1, \tag{2.16}$$

the pressure term in (2.11) is

$$\frac{\partial}{\partial s}\left[\!\left[\frac{p}{\rho}\right]\!\right] = -\frac{2}{\rho_2}\left[\!\left[\mu\frac{\partial^2}{\partial s^2}(\boldsymbol{u}\cdot\hat{\boldsymbol{t}})\right]\!\right] - \frac{1}{\rho_2}\frac{\partial}{\partial s}(T\kappa) + \left[\!\left[\frac{1}{\rho}\right]\!\right]\frac{\partial p_1}{\partial s}. \tag{2.17}$$

Hence, for flows that fulfil the pressure boundary condition, a variation of the product of surface tension and curvature along the interface acts as a source of vorticity.

2.2. *Conservation of vorticity/circulation*

Part of the motivation for this article is the observation, in free-surface flows, that vorticity can seem to disappear (e.g. in the wake of a circular cylinder close to a free surface (Sheridan *et al.* 1997; Reichl *et al.* 2005)). Some authors have appeared comfortable with the notion that the total vorticity (circulation) need not be conserved (Rood 1994; Wu & Wu 1996), whilst others have included the vortex sheet at the free surface for conservation of circulation (Lundgren & Koumoutsakos 1999). Here, we demonstrate the general principle of vorticity conservation, acknowledging that the property of conservation in a physical quantity such as vorticity or circulation provides a powerful analytical tool.

Integrating (2.11) along the interface, we obtain

$$\int_a^b [\![\sigma]\!]\,\mathrm{d}s = \int_a^b \frac{\mathrm{d}\gamma}{\mathrm{d}t}\,\mathrm{d}s + \left(\left[\!\left[\frac{p}{\rho}\right]\!\right]_b - \left[\!\left[\frac{p}{\rho}\right]\!\right]_a\right) + \int_a^b \kappa\,[\![(\boldsymbol{u}\cdot\hat{\boldsymbol{n}})(\boldsymbol{u}\cdot\hat{\boldsymbol{t}})]\!]\,\mathrm{d}s. \tag{2.18}$$

Inserting (2.18) into (2.6), we get

$$\frac{\mathrm{d}}{\mathrm{d}t}\left(\int_A \omega\,\mathrm{d}A + \int_a^b \gamma\,\mathrm{d}s\right) = \oint_C \nu\boldsymbol{\nabla}\omega\cdot\boldsymbol{n}\,\mathrm{d}s - \left(\left[\!\left[\frac{p}{\rho}\right]\!\right]_b - \left[\!\left[\frac{p}{\rho}\right]\!\right]_a\right) - \int_a^b \kappa\,[\![(\boldsymbol{u}\cdot\hat{\boldsymbol{n}})(\boldsymbol{u}\cdot\hat{\boldsymbol{t}})]\!]\,\mathrm{d}s. \tag{2.19}$$

If all the terms on the right of (2.19) are zero, the total vorticity in the fluid region A is constant in the sense that

$$\int_A \omega\,\mathrm{d}A + \int_a^b \gamma\,\mathrm{d}s = \text{const.} \tag{2.20}$$

The second term on the left represents the circulation contained in the interface. Consider the circuit consisting of C_1' and C_2' connected by two short segments crossing the interface through $\boldsymbol{a}$ and $\boldsymbol{b}$. The circulation of this circuit in the limit where C_1' and C_2' approach the interface I is $\int_a^b \gamma\,\mathrm{d}s$. Here, γ therefore appears as the linear circulation density of the interface. If one includes the circulation stored in the vortex sheet at the interface in the balance, (2.20) expresses the conservation of the total circulation in the fluid. It is easy to envisage such a situation. For example, if the fluid domain is unbounded, so that there is no vorticity flux into A, and all interfaces that might exist are closed ($\boldsymbol{a}=\boldsymbol{b}$) and steady, then (2.20) holds. Another case is given by an unbounded (steady) interface, whose properties are the same in the limits going in each direction. In § 3 we will see examples of such flows.

To reiterate, in the case of an interface or boundary with free slip, a vortex sheet model is not imposed, but rather arises from the imposition of zero tangential shear stress. In the case of a curved boundary with zero tangential shear stress, the condition of solid-body rotation means that a viscous boundary layer can appear adjacent to the vortex sheet at the interface.

The results we have obtained until now depend only on the fluids being incompressible and evolving according to the Navier–Stokes equations. We now examine the role played by different boundary conditions at the interface.

2.3. *No-slip interface*

If the no-slip condition $[\![\boldsymbol{u}]\!] = \boldsymbol{0}$ is imposed at the interface, the expressions above simplify significantly. The vorticity source density given by (2.11) reduces to

$$[\![\sigma]\!] = \frac{\partial}{\partial s}\left[\!\!\left[\frac{p}{\rho}\right]\!\!\right], \tag{2.21}$$

and, if the pressure boundary condition holds, (2.17) becomes

$$\frac{\partial}{\partial s}\left[\!\!\left[\frac{p}{\rho}\right]\!\!\right] = -2\frac{[\![\mu]\!]}{\rho_2}\frac{\partial^2}{\partial s^2}(\boldsymbol{u}\cdot\hat{\boldsymbol{t}}) - \frac{1}{\rho_2}\frac{\partial}{\partial s}(T\kappa) + \left[\!\!\left[\frac{1}{\rho}\right]\!\!\right]\frac{\partial p_1}{\partial s}. \tag{2.22}$$

Since $\gamma = [\![\boldsymbol{u}\cdot\hat{\boldsymbol{t}}]\!] = 0$, there is no vorticity stored in the interface and the total vorticity balance (2.19) becomes

$$\frac{\mathrm{d}}{\mathrm{d}t}\left(\int_A \omega\,\mathrm{d}A\right) = \oint_C \nu\nabla\omega\cdot\boldsymbol{n}\,\mathrm{d}s - \left(\left[\!\!\left[\frac{p}{\rho}\right]\!\!\right]_b - \left[\!\!\left[\frac{p}{\rho}\right]\!\!\right]_a\right). \tag{2.23}$$

If the interface is closed, or if $[\![p/\rho]\!]$ takes the same limiting value in both directions of an unbounded interface, the total vorticity (circulation) is conserved in the sense that it can change only if there is a flux at the outer boundary C.

A balance of the vorticity for one fluid can be obtained as follows. If the velocity at the interface, which is single-valued for the no-slip condition, is denoted by $\boldsymbol{U}$, we have from (2.10) that

$$\sigma_1 = \frac{\mathrm{d}}{\mathrm{d}t}(\boldsymbol{U}\cdot\hat{\boldsymbol{t}}) + \frac{1}{\rho_1}\frac{\partial p_1}{\partial s} + \kappa(\boldsymbol{U}\cdot\hat{\boldsymbol{n}})(\boldsymbol{U}\cdot\hat{\boldsymbol{t}}) - \frac{1}{2}\frac{\partial}{\partial s}(\boldsymbol{U}\cdot\hat{\boldsymbol{n}})^2. \tag{2.24}$$

The divergence theorem on A_1 yields directly

$$\frac{\mathrm{d}}{\mathrm{d}t}\int_{A_1}\omega\,\mathrm{d}A = \int_{C_1}\nu\nabla\omega\cdot\boldsymbol{n}\,\mathrm{d}s + \int_a^b \sigma_1\,\mathrm{d}s. \tag{2.25}$$

Inserting σ_1 from (2.24) into (2.25), we get

$$\begin{aligned}\frac{\mathrm{d}}{\mathrm{d}t}\int_{A_1}\omega\,\mathrm{d}A \;=\; &\int_{C_1}\nu\nabla\omega\cdot\boldsymbol{n}\,\mathrm{d}s + \frac{\mathrm{d}}{\mathrm{d}t}\int_a^b \boldsymbol{U}\cdot\hat{\boldsymbol{t}}\,\mathrm{d}s + \left(\left.\frac{p_1}{\rho_1}\right|_b - \left.\frac{p_1}{\rho_1}\right|_a\right)\\ &+ \int_a^b \kappa(\boldsymbol{U}\cdot\hat{\boldsymbol{n}})(\boldsymbol{U}\cdot\hat{\boldsymbol{t}})\,\mathrm{d}s - \frac{1}{2}\left[(\boldsymbol{U}\cdot\hat{\boldsymbol{n}})_b^2 - (\boldsymbol{U}\cdot\hat{\boldsymbol{n}})_a^2\right].\end{aligned} \tag{2.26}$$

Thus, vorticity flows into a fluid at a no-slip interface due to tangential acceleration and pressure gradients along the interface, as well as from effects related to the normal motion of the interface and its curvature.

The limit $\nu_2 \to \infty$, in which fluid 2 is a rigid body (i.e. a solid), can be treated within the present framework. In that case, the vorticity in fluid 2 is independent of the position,

$$\omega = 2\Omega_0, \tag{2.27}$$

where Ω_0 is the angular velocity of the body. Then the vorticity balance (2.23) can be rewritten as

$$\frac{\mathrm{d}}{\mathrm{d}t}\left(\int_{A_1}\omega\,\mathrm{d}A + 2\Omega_0\,\mathrm{Area}(A_2)\right) = \oint_C \nu\nabla\omega\cdot\boldsymbol{n}\,\mathrm{d}s - \left(\left[\!\!\left[\frac{p}{\rho}\right]\!\!\right]_b - \left[\!\!\left[\frac{p}{\rho}\right]\!\!\right]_a\right). \tag{2.28}$$

When the solid body is of finite size and entirely located within the contour C of the control volume, the interface I is closed and (2.28) reduces to

$$\frac{\mathrm{d}}{\mathrm{d}t}\left(\int_{A_1}\omega\,\mathrm{d}A + 2\Omega_0\,\mathrm{Area}(A_2)\right) = \oint_C \nu\nabla\omega\cdot\boldsymbol{n}\,\mathrm{d}s. \tag{2.29}$$

2.4. *Stress-free interface*

At the interface of two viscous fluids, one normally imposes dynamical boundary conditions: it is assumed that the tangential and normal stresses vary continuously across the interface. A free surface of fluid 1 occurs when fluid 2 is unable to sustain any tangential stress (Brøns 1994; Sarpkaya 1996). We can accommodate this situation here by simply assuming fluid 2 to be inviscid, with $\nu_2 = 0$. This implies that $\sigma_2 = 0$, so that there is no vorticity flux into or out of fluid 2. However, vorticity can still be exchanged between the interface and fluid 1 via a non-zero σ_1.

From (2.10) we have for fluid 1

$$\sigma_1 = \frac{\mathrm{d}}{\mathrm{d}t}(\boldsymbol{u}_1\cdot\hat{\boldsymbol{t}}) + \frac{1}{\rho_1}\frac{\partial p_1}{\partial s} + \kappa(\boldsymbol{u}_1\cdot\hat{\boldsymbol{n}})(\boldsymbol{u}_1\cdot\hat{\boldsymbol{t}}) - \frac{1}{2}\frac{\partial}{\partial s}(\boldsymbol{u}_1\cdot\hat{\boldsymbol{n}})^2. \tag{2.30}$$

If one further imposes the pressure boundary condition, assuming that the constant pressure in fluid 2 is $p_2 = 0$, (2.13) becomes

$$p_1 = \mu_1\,\hat{\boldsymbol{n}}\cdot\boldsymbol{D}\cdot\hat{\boldsymbol{n}} + T\kappa = -2\mu_1\left(\frac{\partial}{\partial s}(\boldsymbol{u}_1\cdot\hat{\boldsymbol{t}}) + \kappa\boldsymbol{u}\cdot\hat{\boldsymbol{n}}\right) + T\kappa, \tag{2.31}$$

from which the pressure term in (2.30) can be rewritten as

$$\frac{1}{\rho_1}\frac{\partial p_1}{\partial s} = -2\nu_1\left(\frac{\partial^2}{\partial s^2}(\boldsymbol{u}\cdot\hat{\boldsymbol{t}}) + \frac{\partial}{\partial s}(\kappa\boldsymbol{u}\cdot\hat{\boldsymbol{n}})\right) + \frac{\partial}{\partial s}(T\kappa). \tag{2.32}$$

Again we see that variation of $T\kappa$ along the interface gives rise to a production of vorticity.

Using the divergence theorem (2.25) on A_1, we get

$$\begin{aligned}\frac{\mathrm{d}}{\mathrm{d}t}\int_{A_1}\omega\,\mathrm{d}A \;=\; &\int_{C_1}\nu\nabla\omega\cdot\boldsymbol{n}\,\mathrm{d}s + \frac{\mathrm{d}}{\mathrm{d}t}\int_a^b \boldsymbol{u}_1\cdot\hat{\boldsymbol{t}}\,\mathrm{d}s + \left(\frac{p_1}{\rho_1}\bigg|_b - \frac{p_1}{\rho_1}\bigg|_a\right)\\ &+ \int_a^b \kappa(\boldsymbol{u}_1\cdot\hat{\boldsymbol{n}})(\boldsymbol{u}_1\cdot\hat{\boldsymbol{t}})\,\mathrm{d}s - \frac{1}{2}\left[(\boldsymbol{u}_1\cdot\hat{\boldsymbol{n}})_b^2 - (\boldsymbol{u}_1\cdot\hat{\boldsymbol{n}})_a^2\right].\end{aligned} \tag{2.33}$$

In fluid 1, there is no constraint on the velocity in the limit approaching the interface. However, from the dynamical boundary condition (zero tangential stress at the interface), the following relation can be derived (Lundgren & Koumoutsakos 1999, their equation (11)):

$$\omega_1 = 2\kappa\boldsymbol{u}_1\cdot\hat{\boldsymbol{t}} - 2\frac{\partial}{\partial s}(\boldsymbol{u}_1\cdot\hat{\boldsymbol{n}}). \tag{2.34}$$

For zero normal motion of the surface, (2.34) reduces to the familiar statement that 'surface vorticity is twice the curvature times tangential velocity', and it follows that

the surface is pointwise in solid-body rotation with angular velocity $\Omega = \boldsymbol{u}_1 \cdot \hat{\boldsymbol{t}}/R$, where $R = 1/\kappa$ is the radius of curvature, since

$$\omega_1 = 2\frac{\boldsymbol{u}_1 \cdot \hat{\boldsymbol{t}}}{R} = 2\Omega. \tag{2.35}$$

In general, for a curved surface with a stress-free boundary condition, the exchange of vorticity between the body of the fluid and the vortex sheet representing this surface is such that the fluid at the surface is in solid-body rotation. In the case of a flat surface, the radius of curvature is infinite and the vorticity at the surface is identically zero. It will be seen in examples later that a curved stress-free surface can lead to active and substantial vorticity introduction into the body of the fluid from the interface.

With (2.34), the vorticity source density (2.30) can be rewritten as

$$\sigma_1 = \frac{\mathrm{d}}{\mathrm{d}t}(\boldsymbol{u}_1 \cdot \hat{\boldsymbol{t}}) + \frac{1}{\rho_1}\frac{\partial p_1}{\partial s} - \frac{1}{2}(\boldsymbol{u}_1 \cdot \hat{\boldsymbol{n}})\omega_1, \tag{2.36}$$

and (2.33) becomes

$$\frac{\mathrm{d}}{\mathrm{d}t}\left(\int_{A_1} \omega \,\mathrm{d}A + \int_a^b \boldsymbol{u}_1 \cdot \hat{\boldsymbol{t}}\,\mathrm{d}s\right) = \int_{C_1} \nu \nabla\omega \cdot \boldsymbol{n}\,\mathrm{d}s + \left(\frac{p_1}{\rho_1}\bigg|_b - \frac{p_1}{\rho_1}\bigg|_a\right) - \frac{1}{2}\int_a^b \kappa(\boldsymbol{u}_1 \cdot \hat{\boldsymbol{n}})\omega_1 \,\mathrm{d}s. \tag{2.37}$$

This means that vorticity is generated from a net pressure gradient in the fluid along the surface as well as from normal motion of the surface. If the tangential velocity at the surface is non-zero, circulation is stored there (second term in brackets on the left).

2.5. *Summary of theoretical findings*

In the above formulation and discussion, and from previous analyses, there are a number of important theoretical findings that will prove useful when analysing and interpreting vorticity generation, diffusion and conservation in various configurations.

For a given (material) control volume, which may contain an interface between two fluids or a boundary with a solid body or an inviscid medium, we note the following:

(*a*) The total circulation only varies due to vorticity flowing into or out of the outer boundary of the control volume through viscous diffusion.

(*b*) Within the fluid, the magnitude of vorticity changes locally due to viscous diffusion and advection, and cross-annihilation of opposite-signed vorticity.

(*c*) Vorticity may be generated at a stationary interface or boundary due to a jump in the tangential acceleration or tangential pressure gradient. The corresponding circulation is 'stored' at the interface in the form of a vortex sheet (velocity jump) and must be included in the overall circulation balance.

(*d*) Normal motion of an interface leads to vorticity generation if the interface is curved and if there is also non-zero tangential motion.

(*e*) At a curved stress-free boundary, the flow at the fluid surface is locally that of solid-body rotation (with zero vorticity for a flat surface). Vorticity is exchanged between the vortex sheet representing the interface and the fluid surface in order to maintain this solid-body rotation.

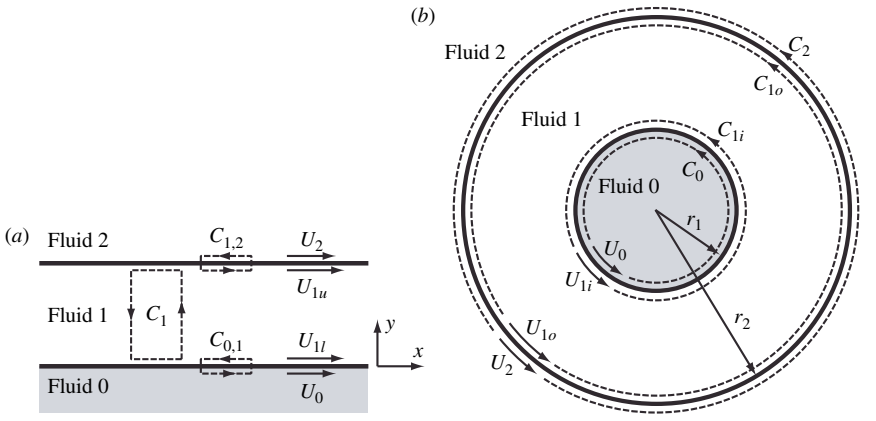

FIGURE 3. Integration paths (dashed lines) for the calculation of (*a*) the linear circulation density in planar flows, with the paths covering a unit length in the x-direction, and (*b*) the circulation for axisymmetric flows. The paths C run along the edges of a given fluid region. The U with the same subscript are the corresponding limit values of the velocity when approaching the relevant interface.

3. Application to planar and axisymmetric flows

We now turn to a number of examples involving different fluids, and including no-slip and stress-free boundary conditions, in order to demonstrate the practical application of the above formulations and concepts.

Two basic two-dimensional configurations are considered: planar flow and axisymmetric flow. Before proceeding to the various examples, we briefly discuss the circulation distribution in these geometries. It will be important to distinguish between the circulation in the body of the fluid and that existing across the interfaces, particularly for stress-free boundaries. In the following, Γ_i denotes the circulation in the body of fluid i, and γ_{ij} the circulation across the interface between fluids i and j. Circulations are calculated along integration paths C according to (2.1), which are shown in figure 3 for the two geometries: C_1 for the main body of fluid (fluid 1), $C_{0,1}$ and $C_{1,2}$ across the lower and upper interfaces for planar flow; and C_0, C_{1i}, C_{1o} and C_2 along the inner and outer interfaces for axisymmetric flow.

In all of the following examples, fluid 0 is of infinite viscosity (i.e. a solid), and the boundary condition is one of no slip: $U_0 = U_{1l}$ or $U_0 = U_{1i}$. Also, in all cases, fluid 2 remains at rest ($U_2 = 0$); it is either a fixed solid, or an inviscid fluid to which no motion can be transferred due to the stress-free boundary condition.

For planar flow (figure 3*a*), the circulations (per unit length in the x direction) in the main body of the fluid of interest (fluid 1) and at the two interfaces are given by:

planar flow circulations

$$\frac{\mathrm{d}\Gamma_1}{\mathrm{d}x} = U_0 - U_{1u}, \quad \frac{\mathrm{d}\gamma_{0,1}}{\mathrm{d}x} = 0, \quad \frac{\mathrm{d}\gamma_{1,2}}{\mathrm{d}x} = U_{1u}, \quad \frac{\mathrm{d}\Gamma_{total}}{\mathrm{d}x} = U_0. \tag{3.1}$$

For the axisymmetric case (figure 3*b*), the various circulations are given by:

axisymmetric flow circulations

$$\Gamma_0 = 2\pi r_1 U_0, \quad \Gamma_1 = 2\pi(r_2 U_{1o} - r_1 U_0), \quad \Gamma_2 = \Gamma_{total} = 0, \quad \gamma_{0,1} = 0, \quad \gamma_{1,2} = -2\pi r_2 U_{1o}. \tag{3.2}$$

3.1. *Planar flows*

In the planar case, there exist two limiting steady solutions admitted by the Navier–Stokes and Helmholtz equations: plug flow (constant velocity, zero vorticity) and uniform shear flow (constant velocity gradient normal to the flow, i.e. constant vorticity). Any steady solution (subscript ∞) must be a combination of the two: $u_\infty = Ay + B$ and $\omega_\infty = -A$, where A and B are constants. These solutions are such that no gradients in the vorticity field remain to further diffuse vorticity.

3.1.1. *Impulsively started flows*

We now consider flows generated by the impulsive motion of a solid no-slip wall. The wall is planar and coincides with the x-axis. At time $t = 0$, the fluid is at rest and the wall is impulsively accelerated to a linear velocity U_0. We consider fluids of both semi-infinite and finite extent, in the latter case being bounded by a steady no-slip boundary or a no-stress boundary at $y = h$. The flow is assumed to remain parallel to the wall at all times: $u = u(y, t), \quad v = 0$.

Table 1 summarises the analytical solutions that can be obtained for these configurations. In all cases, the instantaneous velocity consists of a limiting steady flow u_∞ plus a transient term u_T, and likewise for the vorticity. The unbounded planar flow is the classical solution found by Stewartson (1951). The planar bounded solutions are easily found by Fourier series methods (Rood 1994).

The evolutions of the velocity and vorticity profiles are further illustrated by numerically solving the velocity equation in table 1, using a standard finite-difference approach and the appropriate boundary conditions corresponding to each case. Second-order central differences were used for the spatial derivatives, with time stepping based on the implicit Crank–Nicolson approach. For the case with a semi-infinite spatial domain, the y-coordinate was transformed using a mapping based on the tangent function, so that a uniform grid could be used in the computational space. Typically, 101 points were used for the grid resolution in the y-direction, noting that doubling the resolution resulted in a negligible change to the predicted velocity field (considerably less than 1 %). Since an implicit time-stepping method was used, there was no restriction on the time step, but again a temporal resolution study was performed to ensure time-step independence of the final results, shown in figure 4.

In all cases, the lower solid boundary has (infinite) tangential acceleration only at $t = 0$. Since there are no tangential pressure gradients, there is no flux of vorticity into the fluid at $t > 0$; all vorticity is introduced from the boundary at $t = 0$. The vorticity flux into the fluid is given by $\sigma_1 = \mathrm{d}U/\mathrm{d}t$ according to (2.24). This acceleration, and hence the vorticity, has the same sign as U_0. For an impulsive acceleration, the vorticity at the surface is singular but the net circulation generated (per unit axial length) is just U_0. The fluid being incompressible, it instantaneously adjusts everywhere to this shearing, leading to vorticity being present at all finite distances but with the bulk in a very thin layer at the boundary at small times. (In the case of a compressible fluid, the outward flow of vorticity will be limited by the local speed of sound.)

(i) Unbounded fluid

For the case of a semi-infinite fluid above an impulsively accelerated plate, all the vorticity is generated at $t = 0$ at the plate, from which it subsequently diffuses away, tending in the limit $t \to \infty$ towards a homogeneous distribution. Since there is only a finite circulation per unit length ($\mathrm{d}\Gamma_{total}/\mathrm{d}x = U_0$ according to (3.1)) to be spread over a semi-infinite domain, the only limiting solution is the one where the vorticity at

Planar flow

Velocity equation: $\dfrac{\partial u}{\partial t} = \nu \dfrac{\partial^2 u}{\partial y^2}$

Initial conditions: $u(y=0, t=0) = U_0, \quad u(y>0, t=0) = 0$

Transient solution: $u_T, \quad \omega_T$

Solution for $t \to \infty$: $u_\infty = Ay + B, \quad \omega_\infty = -A$

General solution: $u = u_\infty + u_T, \quad \omega = \omega_\infty + \omega_T$

(*a*) Unbounded

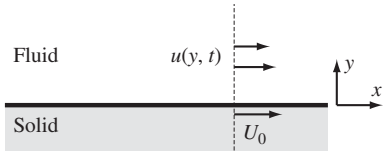

$$A = 0, \quad B = U_0$$

$$u_T = -\frac{2U_0}{\sqrt{\pi}} \int_0^s \mathrm{e}^{-\phi^2}\, \mathrm{d}\phi, \quad s = \frac{y}{2\sqrt{\nu t}}$$

$$\omega_T = \frac{U_0}{\sqrt{\pi \nu t}}\, \mathrm{e}^{-s^2}$$

(*b*)

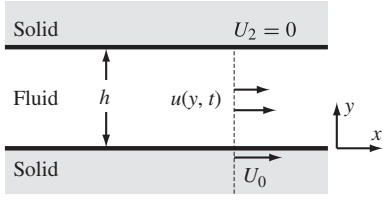

$$A = -\frac{U_0}{h}, \quad B = U_0$$

$$u_T = -\frac{2U_0}{\pi} \sum_{k=1}^{\infty} \frac{1}{k}\, \mathrm{e}^{-\lambda_k^2 \nu t} \sin \lambda_k y, \quad \lambda_k = \frac{\pi k}{h}$$

$$\omega_T = \frac{2U_0}{h} \sum_{k=1}^{\infty} \mathrm{e}^{-\lambda_k^2 \nu t} \cos \lambda_k y$$

(*c*)

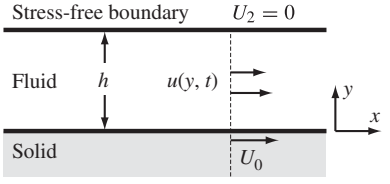

$$A = 0, \quad B = U_0$$

$$u_T = -\frac{4U_0}{\pi} \sum_{k=0}^{\infty} \frac{1}{1+2k}\, \mathrm{e}^{-\lambda_k^2 \nu t} \sin \lambda_k y, \quad \lambda_k = \frac{\pi(1+2k)}{2h}$$

$$\omega_T = \frac{2U_0}{h} \sum_{k=0}^{\infty} \mathrm{e}^{-\lambda_k^2 \nu t} \cos \lambda_k y$$

TABLE 1. Flow generated from rest by the impulsive motion (with velocity U_0) of a flat plate in its own plane, without tangential pressure gradients, showing schematics (left) and analytical solutions (right): (*a*) unbounded fluid above; (*b*) fluid layer bounded above by a stationary solid wall; and (*c*) fluid layer bounded above by a stress-free interface. Here, A and B are constants.

any finite distance approaches zero. Given the no-slip condition at the plate surface, the fluid at $y = 0$ must have velocity U_0, and the fluid approaches a plug flow with uniform velocity (see table 1*a*). The corresponding evolution of the velocity and vorticity profiles can be seen in figure 4(*a*). The total vorticity (circulation) in the entire semi-infinite domain is nevertheless conserved.

(ii) No-slip upper boundary

For a layer of fluid with a no-slip condition at its upper surface, the vorticity also diffuses away from its initial concentration at the impulsively accelerated plate. In

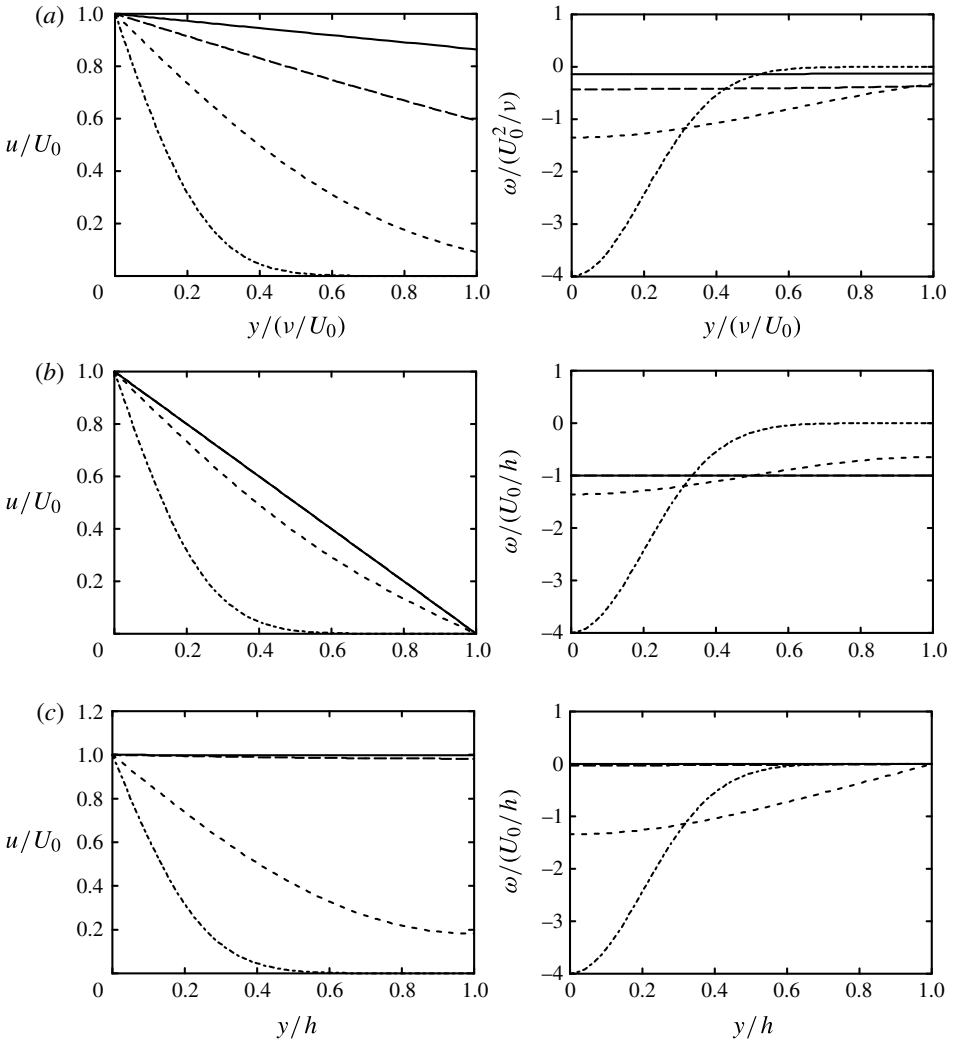

FIGURE 4. Transient velocity (left) and vorticity (right) for an impulsively accelerated flat plate, for the three cases shown in table 1: (*a*) unbounded fluid; (*b*) fluid layer bounded by a solid body at rest; (*c*) fluid layer bounded by a stress-free interface. Line types denote different non-dimensional times $\tau = tU_0/h$ (bounded) or $\tau = tU_0^2/\nu$ (unbounded): $\tau = 0.01$ (dotted), $\tau = 0.1$ (short dashed), $\tau = 1$ (long dashed) and $\tau = 10$ (solid). To enable a meaningful comparison between the unbounded and bounded cases, the Reynolds number in the latter is set to $Re = U_0 h/\nu = 1$.

this case, it cannot flow into the top interface, which is unable to support a velocity jump; all of the initially generated vorticity must remain in the body of the fluid. The only limiting solution available is one where the vorticity is uniformly distributed and a flow with constant shear (normal velocity gradient) is obtained (see table 1*b* and figure 4*b*).

(iii) Stress-free upper boundary

In the case of a layer of fluid with a stress-free condition at the top, the vorticity initially evolves similarly to the previous two cases. It again diffuses away from where

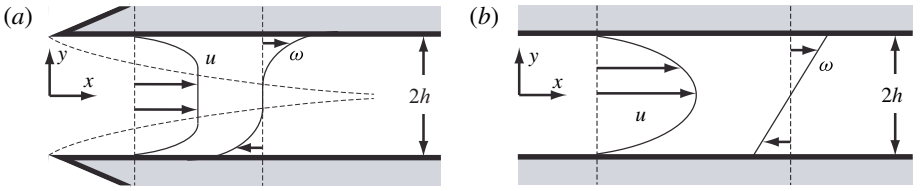

FIGURE 5. Schematic of Poiseuille flow: (*a*) inlet and (*b*) fully developed.

it is initially generated by the plate (at $y = 0$), but this time the fluid at the upper interface is free to move. The upward diffusion continues until no vorticity remains in the body of the fluid, i.e. until a plug flow with constant velocity U_0 is obtained (see table 1*c*). The circulation is then entirely stored at the free surface in the form of a vortex sheet (velocity jump). Typical instantaneous profiles are shown in figure 4(*c*).

In summary, very different outcomes for the final distribution of the vorticity are obtained, depending on the upper boundary condition: zero vorticity in the body of the fluid (i.e. plug flows) for the semi-infinite and stress-free boundary cases, and uniform vorticity (i.e. constant velocity shear) for the no-slip boundary case. In all configurations, all the vorticity is generated at the initial instant, and the total circulation remains constant thereafter.

These observations may be compared with a description in terms of momentum, which in turn does not remain constant. At the initial instant, owing to the no-slip condition at the lower boundary, the fluid interface layer is given a non-zero velocity. As time proceeds, momentum is continually transferred into the fluid, with new momentum being generated in the solid due to external forcing needed to keep the velocity of the solid constant. The momentum flux is governed by the wall shear stress τ_w given by

$$\tau_w = \mu \frac{\partial u}{\partial y}(y = 0, t) = -\mu\omega(y = 0, t), \tag{3.3}$$

where μ is the dynamic viscosity of the fluid. It appears from table 1 that the wall stress is never zero. However, in all cases it tends to zero as time goes to infinity.

3.1.2. *Flow with a streamwise pressure gradient: Poiseuille flow*

The examples considered hitherto have in common that there are no tangential pressure gradients. For completeness, we mention a simple and familiar flow configuration where vorticity is generated by pressure gradients: the planar Poiseuille flow (figure 5). This example is considered in detail in Morton (1984); we shall therefore recall only briefly the main results.

When the flow is bounded by planes at $y = \pm h$, and the constant pressure gradient is denoted by p_x, the fully developed Poiseuille flow is given by a parabolic velocity profile

$$u = -\frac{h^2 p_x}{2\mu}\left(1 - \frac{y^2}{h^2}\right), \tag{3.4}$$

and the vorticity is linear in profile

$$\omega = \frac{p_x}{\mu} y. \tag{3.5}$$

The vorticity sources at the bottom and top boundaries are, according to (2.24), $-p_x/\rho$ and p_x/ρ, respectively. Thus amounts of vorticity that are equal in magnitude and opposite in sense flow into the fluid due to the pressure gradient, in accordance with the fact that the total circulation (per unit length) is zero; this can be observed in the growing boundary layers in the inlet flow (figure 5*a*). There is no flux of vorticity out of the boundaries; vorticity of opposite sign cross-annihilate continuously, leading to the steady-state fully developed solution far downstream (figure 5*b*). This cross-annihilation of vorticity provides one of the keys to understanding how vorticity can decay in a flow, in particular in the flow past a submerged cylinder, which motivated our discussion in the introduction.

3.2. *Axisymmetric flows*

In the axisymmetric configurations we consider here, the flow is generated by the rotation of a solid circular cylinder (radius r_1), with a no-slip condition at its surface (see table 2). At $t = 0$, the fluid is at rest, and the wall is impulsively accelerated to an angular velocity Ω_0. Fluids of both infinite and finite extent are considered; in the latter case, the fluid domain is bounded at radius r_2 either by a stationary no-slip wall or by a stress-free interface. The velocity field is assumed to be axisymmetric, with an azimuthal component $u(r, t)$. In all cases (except for the example of an expanding cylinder), the radial velocity is zero.

Table 2 summarises the analytical solutions that can be obtained for the cases where the radius and angular velocity of the inner cylinder remain constant after the initial impulse. As for the planar flows, the instantaneous velocity consists of a limiting steady solution u_∞ plus a transient term u_T, and likewise for the vorticity. The general limiting solution, for which no diffusion gradients exist in the Helmholtz equation (1.2), is a combination of a potential point-vortex flow with zero vorticity and a solid-body rotation with uniform vorticity, i.e. $u_\infty = A/r + Br$ and $\omega_\infty = 2B$, where A and B are constants. The circular flow in an unbounded domain (table 2*a*) was obtained by Mallick (1957).

As described above for the planar geometry, we use numerical solutions of the one-dimensional velocity equation in table 2 (with the appropriate boundary conditions) to illustrate the evolution of the velocity and vorticity profiles in the various cases considered in the following.

3.2.1. *Unbounded flow*

(i) Flow induced by a rotating cylinder

When there is no outer boundary (i.e. $r_2 \to \infty$), the finite vorticity generated initially at the no-slip interface with the solid cylinder diffuses out towards infinity, with the vorticity in the fluid at any finite radius tending to zero in the limit $t \to \infty$. The velocity field tends to that produced by a point vortex having the same circulation as the one contained in the rotating cylinder, with the azimuthal velocity varying inversely with the radius (i.e. from table 2*a*, $u_\infty = \Omega_0 r_1^2/r$). Figures 6(*a*) and 7(*a*) show the evolution of the velocity profiles and vorticity field after the impulsive rotation.

Note that the vorticity generated in the fluid at $t = 0$ is negative, even if the cylinder rotates in the positive direction. This can immediately be understood from the conservation of circulation. Referring to (2.28), where the unbounded fluid is fluid 1, the right-hand side is zero. Thus, the total circulation of the solid–fluid system is constant and equal to zero, the value for $t < 0$. As the cylinder is accelerated to a positive vorticity, the vorticity in the fluid must be negative. The same can be seen

Axisymmetric flow

Velocity equation: $\dfrac{\partial u}{\partial t} = \nu\left[\dfrac{1}{r}\dfrac{\partial}{\partial r}\left(r\dfrac{\partial u}{\partial r}\right) - \dfrac{u}{r^2}\right]$

Initial conditions: $u(r = r_1, t = 0) = \Omega_0 r_1, \quad u(r > r_1, t = 0) = 0$

Transient solution: $u_T, \quad \omega_T$

Solution for $t \to \infty$: $u_\infty = \dfrac{A}{r} + Br, \quad \omega_\infty = 2B$

General solution: $u = u_\infty + u_T, \quad \omega = \omega_\infty + \omega_T$

(*a*)

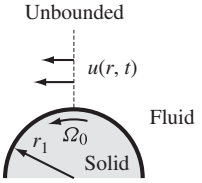

$$A = \Omega_0 r_1^2, \quad B = 0$$

$$u_T = \frac{2r_1\Omega_0}{\pi}\int_0^\infty \frac{\mathrm{J}_1(rx)\mathrm{Y}_1(r_1x) - \mathrm{J}_1(r_1x)\mathrm{Y}_1(rx)}{x[\mathrm{J}_1^2(r_1x) + \mathrm{Y}_1^2(r_1x)]}\,\mathrm{e}^{-x^2\nu t}\,\mathrm{d}x$$

$$\omega_T = \frac{2r_1\Omega_0}{\pi}\int_0^\infty \frac{\mathrm{J}_0(rx)\mathrm{Y}_1(r_1x) - \mathrm{J}_1(r_1x)\mathrm{Y}_0(rx)}{\mathrm{J}_1(r_1x)^2 + \mathrm{Y}_1(r_1x)^2}\,\mathrm{e}^{-x^2\nu t}\,\mathrm{d}x$$

(*b*)

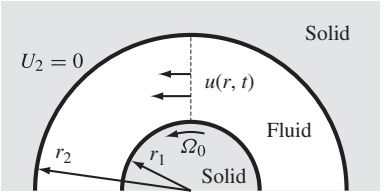

$$A = \frac{\Omega_0 r_1^2 r_2^2}{r_2^2 - r_1^2}, \quad B = -\frac{\Omega_0 r_2^2}{r_2^2 - r_1^2}$$

(*c*)

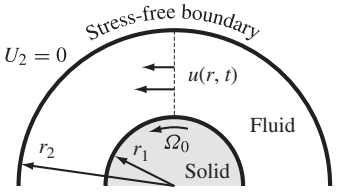

$$A = 0, \quad B = \Omega_0$$

TABLE 2. Flow generated from rest by the impulsive rotation (with angular velocity Ω_0) of a circular cylinder: schematics (left) and analytical solutions (right). (*a*) Unbounded fluid; (*b*) fluid layer bounded by a stationary solid wall; (*c*) fluid layer bounded by a stress-free interface. Here, A and B are constants, and the J_i and Y_i are Bessel functions of the first and second kind, of order i.

from the vorticity flux given in (2.24). The normal vector $\hat{\boldsymbol{n}}$ points into the cylinder such that $\hat{\boldsymbol{n}} = -\boldsymbol{e}_r$ and $\hat{\boldsymbol{t}} = -\boldsymbol{e}_\theta$ and hence $\boldsymbol{U}\cdot\hat{\boldsymbol{t}}$ will be negative.

(ii) Flow induced by a rotating and expanding cylinder

In order to observe the vorticity generation resulting from motion of a boundary in the normal direction, a simple example (not included in table 2) of an expanding rotating cylinder is considered now. This configuration is shown schematically in figure 8. The cylinder initially has a radius R_i and rotates with an angular velocity Ω_i. A no-slip boundary condition is again imposed on the cylinder surface, and the velocity field in the unbounded surrounding fluid is initially irrotational:

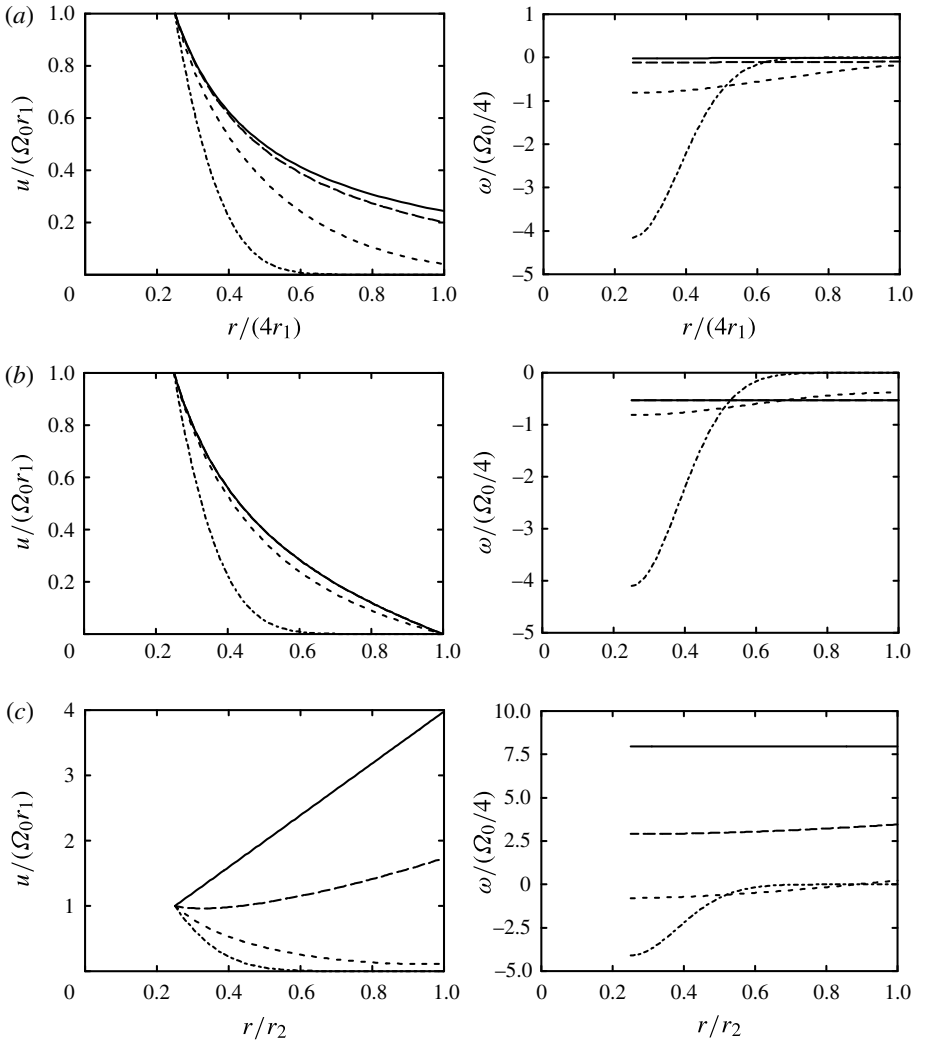

FIGURE 6. Transient velocity (left) and vorticity (right) for an impulsively rotated cylinder, for the three cases shown in table 2, with $r_2 = 4r_1$ and $Re = 4\Omega_0 r_1^2/\nu = 1$: (*a*) unbounded fluid; (*b*) fluid layer bounded by a solid body at rest; (*c*) fluid layer bounded by a stress-free interface. Line types denote different non-dimensional times $\tau = t\Omega_0/4$: $\tau = 0.01$ (dotted), $\tau = 0.1$ (short dashed), $\tau = 1$ (long dashed), $\tau = 10$ (solid).

$u(r, t = 0) = \Omega_i R_i^2/r$. From $t = 0$ onwards, the cylinder radius $R(t)$ is increased, and a time-dependent angular velocity $\Omega(t)$ is imposed. At the cylinder surface, we have $\boldsymbol{U} \cdot \hat{\boldsymbol{t}} = -\Omega R$ and $\boldsymbol{U} \cdot \hat{\boldsymbol{n}} = \mathrm{d}R/\mathrm{d}t$ such that, according to (2.24), there is a vorticity flux into the fluid given by

$$\sigma_1 = \frac{\mathrm{d}}{\mathrm{d}t}(\boldsymbol{U} \cdot \hat{\boldsymbol{t}}) + \kappa(\boldsymbol{U} \cdot \hat{\boldsymbol{n}})(\boldsymbol{U} \cdot \hat{\boldsymbol{t}}) = -\frac{1}{R}\frac{\mathrm{d}}{\mathrm{d}t}(\Omega R^2). \tag{3.6}$$

Figure 9 shows numerically calculated velocity and vorticity profiles for a linearly growing radius of the cylinder. In figure 9(*a*), Ω is held constant, leading to an increasing flux of negative vorticity into the fluid from the cylinder. Both terms

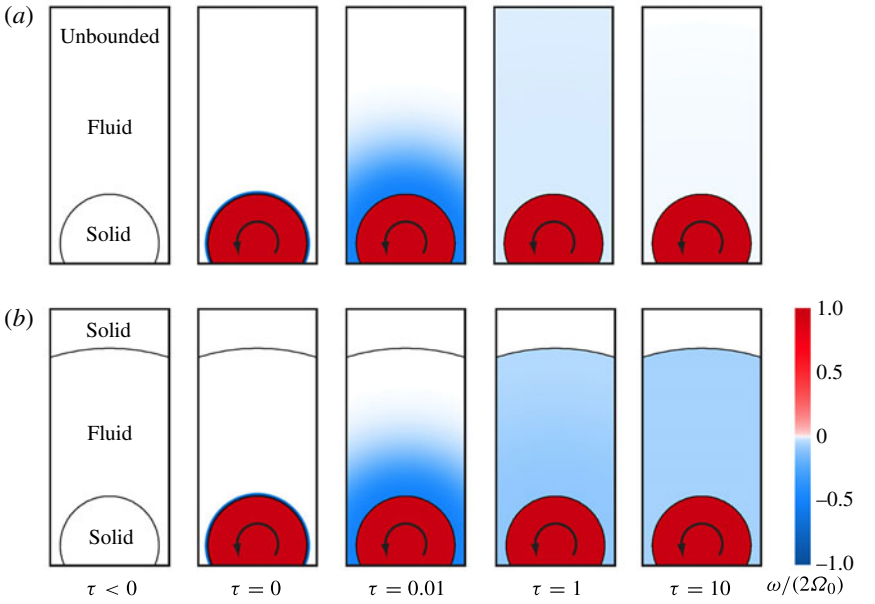

FIGURE 7. (Colour online) Colour contours showing the evolution of the vorticity field in the axisymmetric flow generated by the impulsive rotation of a cylinder: (*a*) unbounded fluid; (*b*) fluid layer bounded by a solid wall. Parameters and data are the same as in figures 6(*a*) and 6(*b*). (If viewing in greyscale please refer to figures 6(*a*) and 6(*b*) to help interpret the colourmap.)

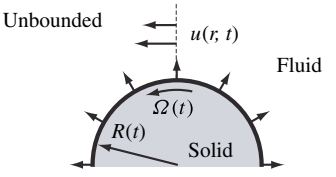

FIGURE 8. Schematic of the expanding rotating cylinder.

$\mathrm{d}(\boldsymbol{U}\cdot\hat{\boldsymbol{t}})/\mathrm{d}t$ and $\kappa(\boldsymbol{U}\cdot\hat{\boldsymbol{n}})(\boldsymbol{U}\cdot\hat{\boldsymbol{t}})$ contribute to the vorticity generation. In figure 9(*b*), ΩR is constant, such that there is no tangential acceleration of the cylinder and the vorticity is generated solely due to the normal motion of the cylinder surface. Finally, in figure 9(*c*), we show the case where ΩR^2 is constant. Then the two sources of vorticity cancel each other exactly, no vorticity enters the flow, and the initial potential flow persists, as expected from (3.6). Note that, in all cases, the total circulation of the system (cylinder plus fluid) remains constant.

3.2.2. *No-slip outer boundary*

When a fixed no-slip boundary is located at a finite radius (r_2 in table 2*b*), the vorticity generated by the impulsive start of the cylinder at $t=0$ is forced to remain within the body of the fluid; no vorticity can flow across or reside in either the inner or the outer no-slip interface, i.e. $\gamma_{0,1}=\gamma_{1,2}=0$ in (3.2). Following the outward diffusion of this vorticity, the flow tends to a combination of solid-body rotation and potential flow in the limit $t\to\infty$, i.e. the classical Taylor–Couette solution. The vorticity is then uniformly distributed in the fluid, with the addition of a point-vortex

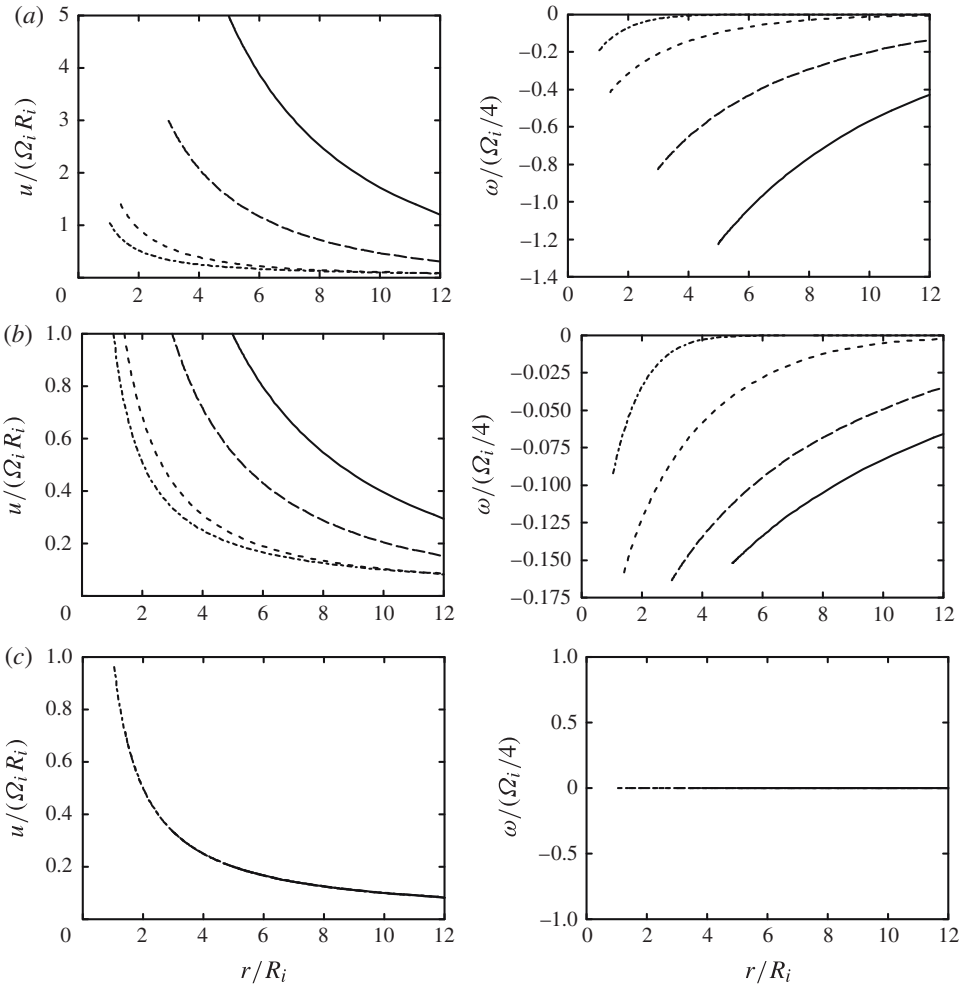

FIGURE 9. Transient velocity (left) and vorticity (right) for a linearly expanding cylinder (figure 8), starting from potential flow, for various time evolutions $\Omega(t)$ of the rotation rate: (*a*) $\Omega = \text{const.}$; (*b*) $\Omega R = \text{const.}$; (*c*) $\Omega R^2 = \text{const}$. Here, R_i and Ω_i are the initial radius and angular velocity of the cylinder, and the Reynolds number is $Re = 4\Omega_i R_i^2/\nu = 1$. The cylinder radius grows according to $R(t) = R_i(1 + \alpha\tau)$, with $\alpha = 0.4$. Line types denote different non-dimensional times $\tau = t\Omega_i/4$: $\tau = 0.1$ (dotted), $\tau = 1$ (short dashed), $\tau = 5$ (long dashed), $\tau = 10$ (solid).

flow due the circulation remaining in the spinning cylinder. From (3.2), with $U_{1o} = 0$, we see that the circulation in the body of the fluid is at all times equal and opposite to that of the cylinder. Figures 6(*b*) and 7(*b*) show the velocity and vorticity distributions at different stages of the flow development, for the example where the outer boundary has a radius of four times that of the cylinder ($r_2 = 4r_1$).

3.2.3. *Stress-free outer boundary*

(i) Forced cylinder

The configuration with a stress-free outer boundary (table 2*c*, figures 6*c* and 10 for a case with $r_2 = 4r_1$) is somewhat unusual in terms of vorticity transport. At first, as

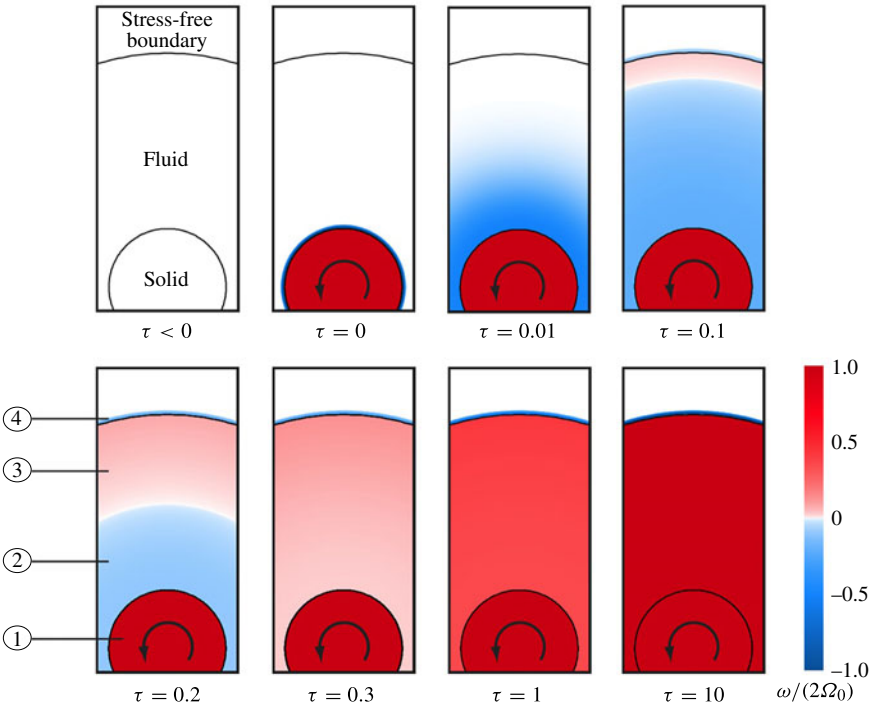

FIGURE 10. (Colour online) Colour contours showing the evolution of the vorticity field in the axisymmetric flow generated by the impulsive rotation of a cylinder, in the presence of a stress-free boundary. Parameters and data are the same as in figure 6(*c*). (If viewing in greyscale please refer to figure 6(*c*) to help interpret the colourmap.)

the viscous stresses accelerate the fluid, the vorticity generated at the cylinder surface begins to diffuse radially outwards, as in the previous cases. In the first instances, the circulation in the fluid body and outer interface is equal and opposite to that of the cylinder: $\Gamma_1 + \gamma_{1,2} = -2\pi r_1 U_0$ from (3.2).

The stress-free condition allows the fluid to accelerate at the outer interface. From (3.2), as U_{1o} increases, the magnitude of negative circulation in the body of the fluid, $\Gamma_1 = 2\pi(r_2 U_{1o} - r_1 U_0)$, decreases, balanced by an increase in the magnitude of the circulation $\gamma_{1,2}$ in the vortex sheet at the outer interface. This is well illustrated in the circulation summary in figure 11, where an exchange of negative vorticity between regions ② and ④ is observed during the time interval $0 < \tau < 0.1$.

However, the stress-free interface forces the flow at the surface to be locally in solid-body rotation: $\omega(r_2) = 2U_{1o}/r_2$ from (2.35). This means that, even though negative vorticity, initially generated at the inner interface, diffuses outwards, vorticity of the opposite sign appears simultaneously at the outer edge of the fluid. Remarkably, the faster the outer edge rotates, due to viscous stresses diffusing the inner negative vorticity outwards, the higher the value of this positive vorticity. No new circulation is created in the system, since the total circulation remains fixed at zero. The generation of positive vorticity in the outer fluid layer is therefore accompanied by an increase of the negative circulation (velocity jump) in the stress-free interface.

The outer positive vorticity flows inwards along the vorticity gradient, gradually cross-annihilating all of the original negative vorticity, and eventually leading to a uniform distribution of positive vorticity, i.e. solid-body rotation, in the fluid (see

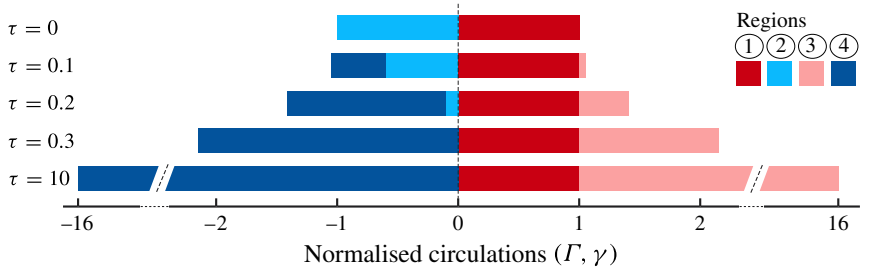

FIGURE 11. (Colour online) Evolution of the circulation contained in the different regions of the axisymmetric flow with a stress-free boundary shown in figures 6(*c*) and 10: ① cylinder with positive circulation Γ_0; ② region with negative vorticity diffusing outwards after the impulsive start of the cylinder; ③ region with positive vorticity spreading inwards from the outer edge of the fluid; and ④ outer interface with negative circulation $\gamma_{1,2}$. All values are normalised using the cylinder circulation $\Gamma_0 = 2\pi r_1^2 \Omega_0$. (If viewing in greyscale please refer to figure 6(*c*) to help interpret the colourmap.)

figures 10 and 11). The equivalent amount of negative circulation remains residing at the outer interface in the form of a vortex sheet. In the final asymptotic state, the individual components of circulation have a very large magnitude, even if their sum is always zero. It should be noted that the angular momentum of the system is not constant, but increases in time, since the cylinder is forced to maintain a constant rotation rate, and angular momentum is transferred to the fluid.

It is tempting to think of a stress-free interface as a passive one. However, whereas it is indeed passive with respect to momentum transfer, it can be extremely active in terms of vorticity, leading to an exchange of vorticity at the fluid surface with circulation residing in the interface. We shall observe later that this is another element to help understand the problem of the 'disappearing' vorticity behind a submerged cylinder.

(ii) Unforced cylinder

A variation of the axisymmetric case with a stress-free outer boundary occurs when the cylinder, rather than being forced to have constant angular velocity for $t > 0$, is allowed to spin down under the frictional resistance of the wall shear stress at the solid–fluid interface (at $r = r_1$ in figure 12*a*), given by

$$\tau_w = \mu r \frac{\partial}{\partial r}\left(\frac{u}{r}\right). \tag{3.7}$$

As in the previous example, the stress-free outer boundary and its concomitant condition of solid-body rotation at the fluid surface determine the final flow. For the cylinder to reach a steady state of rotation, the wall shear stress must vanish, which means that it must be co-rotating with the fluid. The only asymptotic solution where no further evolution takes place as a result of vorticity diffusion is the one with solid-body rotation of the coupled cylinder–fluid system. The time-dependent solutions in figure 12(*b*,*c*), and the vorticity maps in figure 13, obtained with the same initial conditions as for the previous forced configuration, show that this is indeed the case. The constant vorticity observed in the end is of course lower than that for the forced case. As before, the total circulation of the system, including the vortex sheet at the outer interface, remains zero at all times.

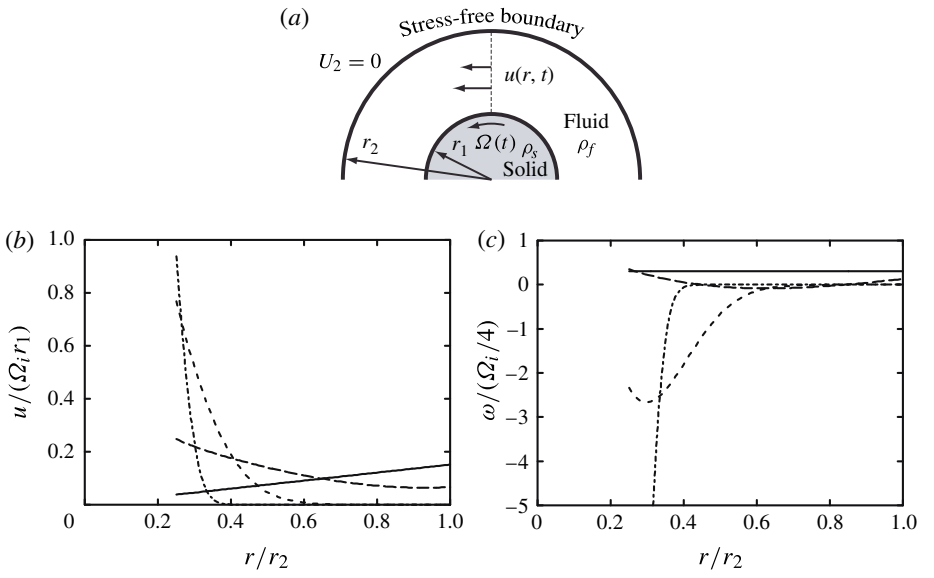

FIGURE 12. Transient axisymmetric flow with a stress-free surface and no external forcing after the initial impulse giving the inner cylinder the angular velocity Ω_i: (*a*) schematic, (*b*) velocity and (*c*) vorticity. Here, $Re = 4\Omega_i r_1^2/\nu = 1$, $r_2 = 4r_1$ and $\rho_s/\rho_f = 10$. Line types denote different non-dimensional times $\tau = t\Omega_i/4$: $\tau = 0.001$ (dotted), $\tau = 0.01$ (short dashed), $\tau = 0.1$ (long dashed), $\tau = 1$ (solid).

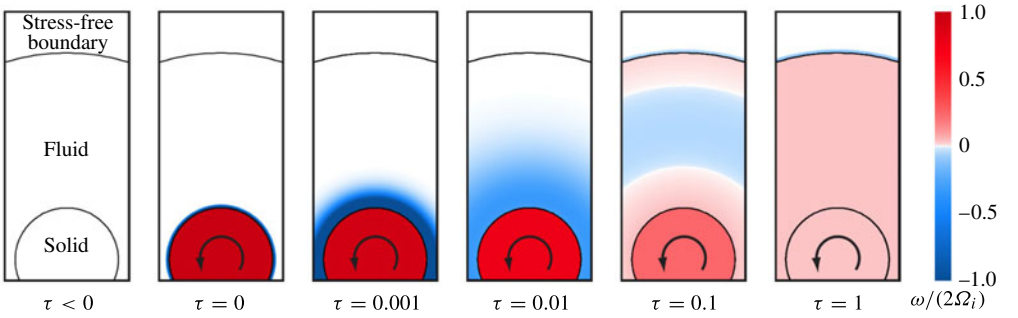

FIGURE 13. (Colour online) Evolution of the vorticity distribution for the unforced cylinder case. Parameters and data are the same as in figure 12(*c*). (If viewing in greyscale please refer to figure 12(*c*) to help interpret the colourmap.)

4. Flow past a circular cylinder near a stress-free surface

We now return to our motivating example given in the introduction, and address the question of where the 'missing' vorticity goes in the wake of a submerged translating cylinder. The flow around a circular cylinder of diameter D, in horizontal motion (velocity U) with respect to a fluid layer having a free surface, depends on three parameters (Sheridan *et al.* 1997; Reichl *et al.* 2005): the Reynolds number $Re = UD/\nu$, the Froude number $Fr = U/\sqrt{gD}$ (g is acceleration due to gravity), and the gap ratio G/D, with G the distance between the top of the cylinder and the position of the unperturbed surface. In the limit $Fr \to 0$, the fluid surface becomes a non-deformable horizontal free-slip (stress-free) interface; we consider this case first.

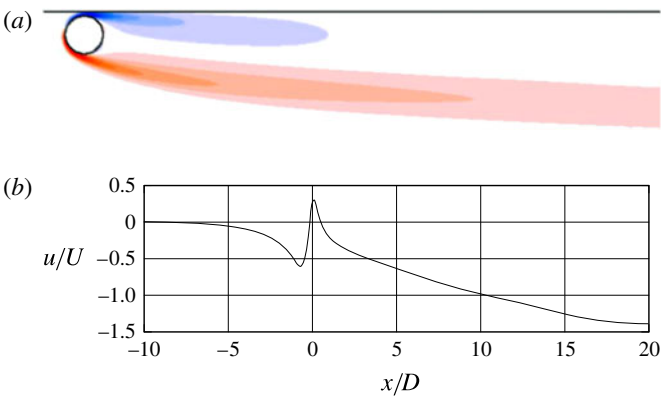

FIGURE 14. (Colour online) (*a*) Predicted long-time vorticity field for flow past a submerged cylinder with a stress-free surface. (*b*) Horizontal velocity at the free surface. Here, $Re = 180$, $Fr = 0$, $G/D = 0.125$. Prediction obtained using an in-house spectral-element code (e.g. Leweke, Thompson & Hourigan 2004; Thompson *et al.* 2006; Thompson, Leweke & Hourigan 2007; Rao *et al.* 2013*a*,*b*).

4.1. *Flat stress-free surface*

The experiments of Sheridan *et al.* (1997) and two-dimensional numerical simulations of Reichl *et al.* (2005) have revealed an intriguing phenomenon when the translating cylinder is moved closer towards the surface. In the case of a zero-Froude-number flow (without surface curvature), the vorticity shed from the upper cylinder surface rapidly disappears as it advects downstream, apparently leading to a net non-zero circulation in the flow, as is clearly shown in figure 1. In addition, and perhaps even more striking, figure 14(*a*) shows the evolution of the vorticity field corresponding to the case shown in figure 1(*b*) at long times. This is quite unlike the Bénard–von Kármán array of alternating vortices (vortex street) forming behind a cylinder in an unbounded free stream. Here, as with the fully submerged case, no net circulation is shed from the cylinder, because its boundary is a closed curve, so that no net pressure gradient can exist – see (2.23). As discussed in the previous sections, vorticity can decay as a result of cross-annihilation with opposite-signed vorticity. Part of the observed decrease of vorticity shed on one side of the cylinder could possibly be explained by cross-annihilation with the vorticity shed from the opposite side of the cylinder. This would, however, still lead to the decay of equal amounts of circulation from each side, without a net imbalance.

The other pertinent finding from the analysis was that vorticity can diffuse towards a stress-free surface and exchange vorticity with the vortex sheet at the interface. The significant change in velocity of the fluid at the free surface (leading to a change in magnitude of the circulation at the interface) demonstrates that this in fact happens. This can be seen in figure 14(*b*), which shows that the downstream velocity at the free surface varies markedly from the zero upstream velocity, i.e. the missing vorticity is stored in a velocity jump across the advecting free surface. However, vorticity is continually shed from the upper part of the cylinder, and therefore continual addition of storage of vorticity is required in the stress-free surface to maintain an imbalance of vorticity in the body of the fluid. Again, this is observed and predicted: the vorticity accumulating at the stress-free interface is continually convected away from

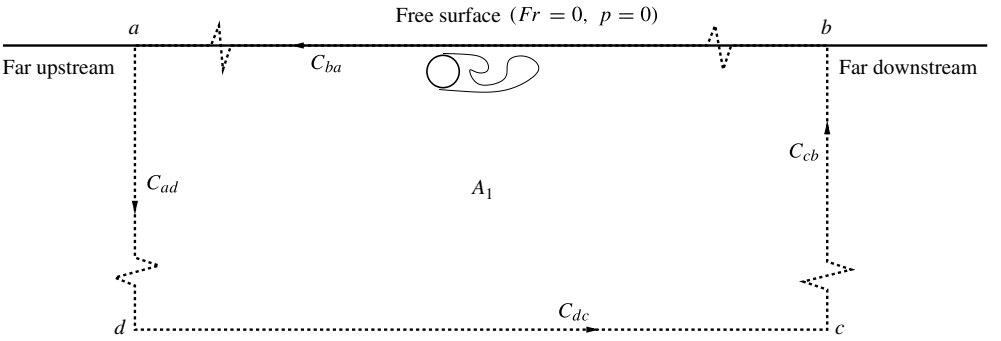

FIGURE 15. Control surface for examining the vorticity balance for the flat stress-free surface problem.

the cylinder since the fluid behind the cylinder is moving to the left more slowly than the cylinder itself.

To investigate this case in more detail, it is instructive to examine the individual terms in the governing equation (2.37) in combination with the arbitrarily selected integration surface shown in figure 15. The two terms on the left are the rate of change of the integrated vorticity in the fluid contained within the surface boundary ($(\mathrm{d}/\mathrm{d}t)\int_{A_1}\omega\,\mathrm{d}A$) and that of the stored circulation at the interface ($(\mathrm{d}/\mathrm{d}t)\int_a^b \boldsymbol{u}_1\cdot\hat{\boldsymbol{t}}\,\mathrm{d}s$), which need to be considered together for vorticity conservation. The right-hand side has three terms: (i) diffusion of vorticity through the surface boundary (excluding the free surface) ($\int_{C_1}\nu\nabla\omega\cdot\boldsymbol{n}\,\mathrm{d}s$); (ii) the pressure difference between the ends of the free-surface contour ($p_1/\rho_1|_b - p_1/\rho_1|_a$); and (iii) a term that is only non-zero for a surface moving normal to itself ($-\frac{1}{2}\int_a^b \kappa(\boldsymbol{u}_1\cdot\hat{\boldsymbol{n}})\omega_1\,\mathrm{d}s$). In this case, if the integration (material) surface extends far upstream and downstream, then (i) the diffusive flux of vorticity through the boundary is zero (since vorticity is only generated at the surface of the cylinder), (ii) the pressure difference term is zero, and (iii) since the surface is stationary, the third term is also zero. Hence the statement of vorticity conservation is that the vorticity generation within the domain A together with the vorticity stored in the vortex sheet at the interface remains a constant. Since the vorticity integral can be reduced to line integrals along the bounding curves using Stokes' theorem, we have

$$\int_{A_1}\omega\,\mathrm{d}A = \int_{C_{ad}}\boldsymbol{u}\cdot\mathrm{d}\boldsymbol{s} + \int_{C_{dc}}\boldsymbol{u}\cdot\mathrm{d}\boldsymbol{s} + \int_{C_{cb}}\boldsymbol{u}\cdot\mathrm{d}\boldsymbol{s} + \int_{C_{ba}}\boldsymbol{u}\cdot\mathrm{d}\boldsymbol{s}. \tag{4.1}$$

Here, the first three terms are zero because the fluid far away from the cylinder remains stationary. The final term varies with time but is equal and opposite to the surface vortex sheet term. Hence, the rate of change of vorticity within the control surface is exactly balanced by the rate of accumulation of vorticity within the vortex sheet at the interface.

Thus, to recap, a closer examination of the flow predictions shows that the deficit in vorticity present in the flow from the disappearing upper shear-layer shedding is balanced precisely by the increase in the circulation of the vortex sheet or velocity jump at the free surface. More generally, according to (2.36), a flux of vorticity to the free-surface interface, in the absence of normal motion, is associated with an acceleration of the fluid surface and/or a pressure gradient along this layer. For an

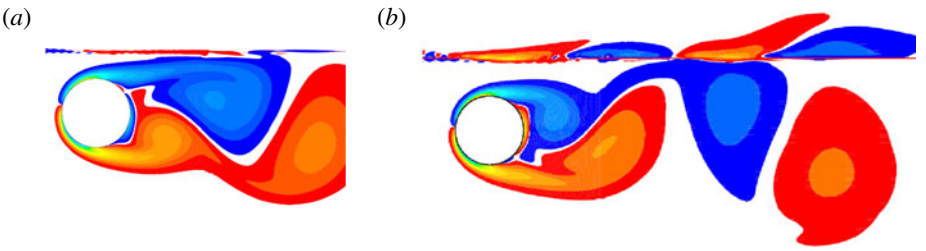

FIGURE 16. (Colour online) Predicted vorticity field for flow past a submerged cylinder for $Re = 180$ and $Fr = 0.2$. (*a*) Surface vorticity for upper fluid with kinematic viscosity ratio (ν_{lower}/ν_{upper}) of 1 and density ratio ($\rho_{lower}/\rho_{upper}$) of 100, for $G/D = 0.4$. (*b*) Vorticity induced in the upper fluid layer when its viscosity is increased to enable greater viscous transport of fluid away from the interface. In this case $G/D = 0.55$. (From Reichl 2001, reproduced with permission.)

initially uniform flow relative to the cylinder, the net pressure difference and the velocity difference at the fluid interface between far upstream and far downstream is zero; therefore, although local vorticity variations can occur and vorticity of one sign seems to 'disappear' into the free surface, overall the circulation is conserved.

In the two-phase predictions of Reichl (2001), where the upper layer of fluid is originally co-moving with the lower layer, the numerical interface between the lower and upper fluids is not precisely sharp – this allows the changes in the vortex sheet to be observed more vividly, as in figure 16(*a*) for (effectively) a stress-free surface. In the case where the upper layer of fluid is more viscous but much lower density, and therefore no longer strictly stress-free, the changes in velocity at the interface induced by the shed vortices manifests as diffusing regions of vorticity (see figure 16*b*). The vortex structures in the lower layer of fluid shed from the cylinder induce vorticity at the surface interface of opposite sign. For a stress-free surface that has no curvature, the vorticity at the fluid surface is maintained at zero through exchange of vorticity with the interface. However, it will be seen that non-zero surface vorticity appears and can separate into the fluid as the Froude number increases and sufficiently high surface curvature forms.

4.2. *Stress-free surface with curvature*

In the case where the stress-free surface is allowed to curve (non-zero Froude number, see figure 17), additional introduction of vorticity into the body of the fluid, balanced by opposite-sign vorticity in the surface vortex sheet, can lead to even more rapid 'disappearance' of vorticity.

The high-speed low-pressure fluid that flows through the gap between the cylinder and the stress-free surface induces circulation at the stress-free interface of sign opposite to that in the separating shear layer. The surface also deflects downwards towards the low-pressure region before curving up towards its original height downstream. Where the stress-free surface curves, the fluid at the surface is compelled to be in solid-body rotation; the resultant vorticity diffuses into the fluid and then separates into the flow from the curved surface further downstream, leading to rapid cross-annihilation of the vorticity shed from the top of the cylinder (see figure 17*b*). (See also Ohring & Lugt (1991) for a related study of the interaction of a vortex pair with a free surface, for which similar behaviours are observed).

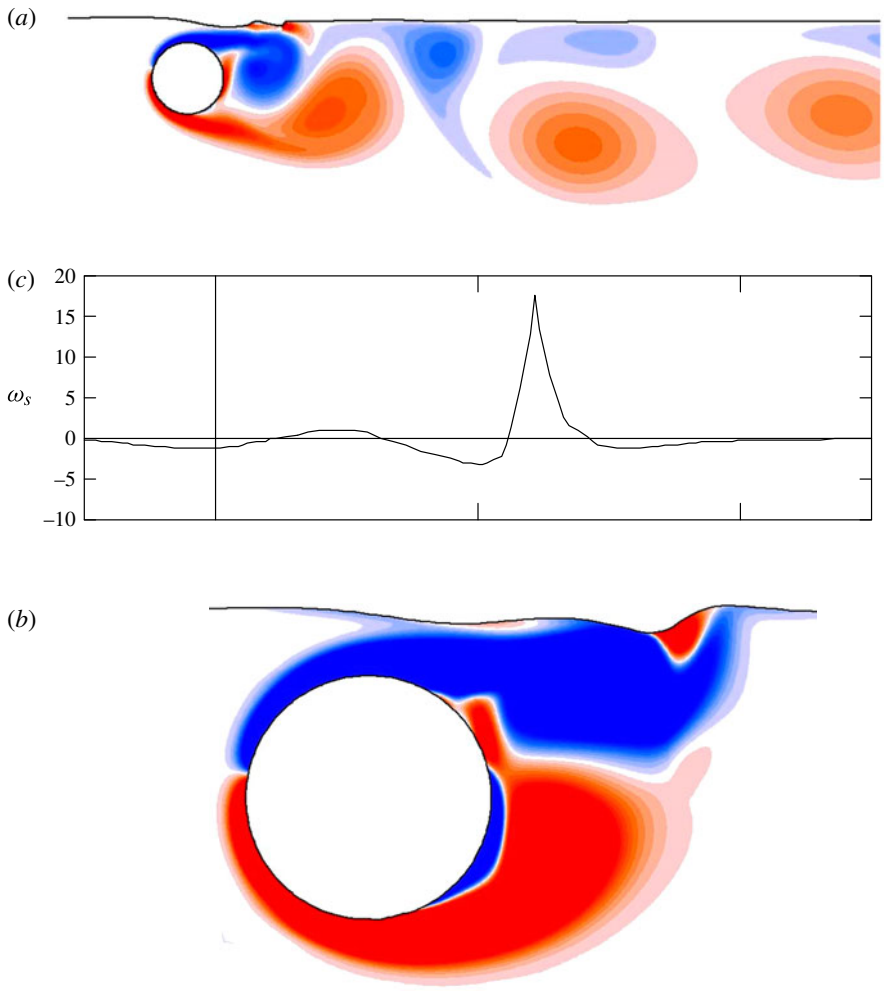

FIGURE 17. (Colour online) Predicted vorticity field for flow past a submerged cylinder when the surface is able to distort; $Re = 180$, $Fr = 0.2$, $G/D = 0.3$. (*a*) Evolved flow after a long time ($t \simeq 24D/U$). (*b*) Vorticity field close to startup ($\Delta t = 0.3D/U$ after the surface is allowed to distort), showing the constraint imposed there on the vorticity by the surface curvature. (*c*) The vorticity along the surface, with negative and positive curvature of the surface clearly associated with negative and positive surface vorticity as specified by (2.35). Again, predictions obtained using an in-house spectral-element code verified on many related problems (e.g. Thompson *et al.* 2006, 2007; Rao *et al.* 2013*a*,*b*; Leweke *et al.* 2004).

We return finally to the two original studies of Sheridan *et al.* (1997) and Reichl *et al.* (2005): the observed and predicted flows for a submerged cylinder in the case of a higher Froude number of 0.6, and similar submerged depths (but differences in Reynolds number) are shown in figure 18. In this case, the curvature of the stress-free surface is even greater and significant amounts of vorticity are exchanged at the curved surface with the vortex sheet at the interface to enforce the flow to be locally in solid-body rotation. Upstream of the cylinder, the stress-free interface

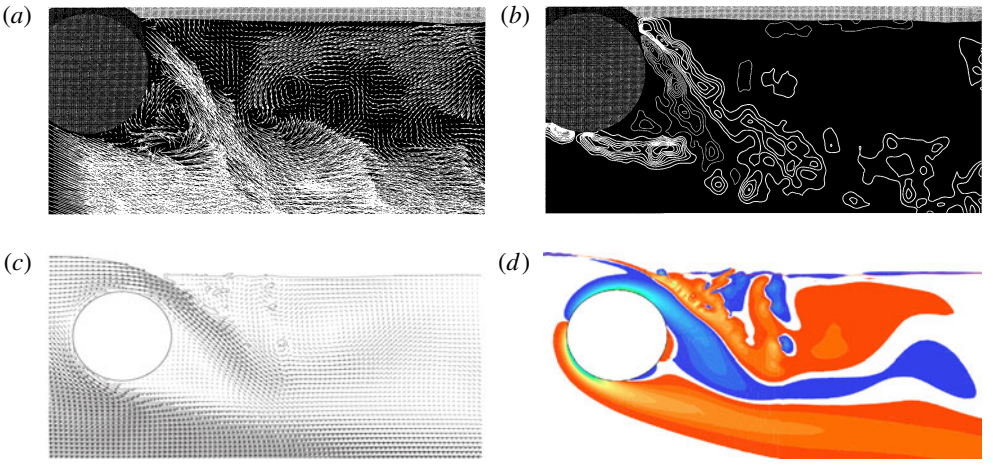

FIGURE 18. (Colour online) Flow around a submerged cylinder for $Fr = 0.6$. (*a*) Velocity and (*b*) vorticity fields from experiments by Sheridan *et al.* (1997) with $G/D = 0.31$ at $Re = O(10^4)$. (*c*) Velocity and (*d*) vorticity fields from two-dimensional simulations by Reichl *et al.* (2005) for $G/D = 0.25$ and $Re = 180$. (All results reproduced with permission.)

begins to curve downwards in a clockwise direction. The solid-body rotation at the fluid surface therefore results in negative vorticity (blue online), which diffuses to form a boundary layer as it flows along the surface. The change in circulation in the interface as the fluid is accelerated through the gap is of the opposite sign (red online). At the interface above the back section of the cylinder, the stress-free interface changes curvature to anticlockwise, with a much smaller radius of curvature. More intense vorticity of positive sign (red online) now appears at the fluid surface to maintain local solid-body rotation. This positive vorticity cannot continue to follow the sharp surface curvature and separates strongly, forming a jet that penetrates deep into the fluid. The negative (blue online) vorticity shed from the upper surface of the cylinder is squeezed between two layers of opposite-sign vorticity and is rapidly cross-annihilated. Downstream at the fluid interface, negative (blue online) vorticity is stored that provides the balance of vorticity to that in the body of the fluid.

5. Conclusions

Vorticity is an important physical quantity in fluid mechanics; it pinpoints the parts of the flow that are often most active in providing fluctuating forces, generating noise and constituting turbulence. Its mathematical definition as the curl of the velocity is simple enough. However, the generation and storage of vorticity at interfaces and boundaries, its transport and decay, and its conservation, are more complex. We have presented here a generalised formulation of the generation, transport and conservation of vorticity and circulation at interfaces between fluids and at boundaries; stark differences are found between no-slip boundaries and stress-free interfaces. Generation of vorticity at an interface or boundary is due to relative acceleration of the fluid(s) or a relative pressure gradient.

The constancy of net vorticity is found in many cases even where the linear or angular momentum of the system is not constant. For example, whenever external

forcing at interfaces is applied only at an instant or for a finite time, the vorticity in the system thereafter is constant even though the linear or angular momentum may continue to vary. This property, and the limited number of final vorticity field states in planar and axisymmetric flows, allows one to determine the final flow, for which no gradients of vorticity can exist. In the case of a planar flow, the limiting flow must be one of uniform vorticity. For an axisymmetric flow, the limiting flow must be a potential flow and/or solid-body rotation. To determine which state will be selected, the condition on the vorticity at the interfaces and/or boundaries are considered: a planar stress-free boundary supports only zero vorticity in the fluid, whereas a no-slip boundary can support non-zero vorticity there; for an axisymmetric stress-free boundary, the vorticity at the fluid surface is set by the tangential velocity and the local boundary/interface curvature, whereas the no-slip boundary/interface can support variable vorticity (but no velocity jump).

The vorticity in the body of a fluid can be exchanged with that at a stress-free interface or boundary and be stored as a vortex sheet (velocity jump). This storage is not possible at a no-slip boundary. Furthermore, tangential fluid motion induced at a curved stress-free boundary results in the appearance of (solid-body rotation) vorticity at the fluid surface, and a balance of opposite-sign vorticity in the interface or boundary vortex sheet. In all cases, vorticity is conserved in the system.

The generation, transport and conservation of vorticity has been demonstrated by a number of examples, including the case of the flow past a cylinder beneath a stress-free surface; the apparent loss in the fluid body of vorticity of one sign shed from the cylinder is precisely balanced by the change in vorticity stored in the interface vortex sheet. Where there is surface curvature, significant amounts of vorticity can form at the fluid surface and in certain cases separate into the flow, leading to rapid cross-annihilation of vorticity shed from the cylinder.

Acknowledgements

This research was supported by Australian Research Council (ARC) Discovery Grants DP0452664, DP110102141 and DP130100822. This paper has been inspired by, and is dedicated to the memory of, Bruce Rutherfurd Morton (1926–2012).

Appendix A. Proof of (2.8)

We have

$$\frac{\mathrm{d}\boldsymbol{u}}{\mathrm{d}t}\cdot\hat{\boldsymbol{t}}=\frac{\mathrm{d}}{\mathrm{d}t}(\boldsymbol{u}\cdot\hat{\boldsymbol{t}})-\boldsymbol{u}\cdot\frac{\mathrm{d}\hat{\boldsymbol{t}}}{\mathrm{d}t}. \tag{A 1}$$

Using the orthogonality of $\hat{\boldsymbol{n}}$ and $\hat{\boldsymbol{t}}$, the last term on the right can be rewritten as

$$\begin{aligned}\boldsymbol{u}\cdot\frac{\mathrm{d}\hat{\boldsymbol{t}}}{\mathrm{d}t} &= \left[(\boldsymbol{u}\cdot\hat{\boldsymbol{n}})\hat{\boldsymbol{n}}+(\boldsymbol{u}\cdot\hat{\boldsymbol{t}})\hat{\boldsymbol{t}}\right]\cdot\left[\left(\frac{\mathrm{d}\hat{\boldsymbol{t}}}{\mathrm{d}t}\cdot\hat{\boldsymbol{n}}\right)\hat{\boldsymbol{n}}+\left(\frac{\mathrm{d}\hat{\boldsymbol{t}}}{\mathrm{d}t}\cdot\hat{\boldsymbol{t}}\right)\hat{\boldsymbol{t}}\right]\\ &= (\boldsymbol{u}\cdot\hat{\boldsymbol{n}})\left(\frac{\mathrm{d}\hat{\boldsymbol{t}}}{\mathrm{d}t}\cdot\hat{\boldsymbol{n}}\right)+(\boldsymbol{u}\cdot\hat{\boldsymbol{t}})\left(\frac{\mathrm{d}\hat{\boldsymbol{t}}}{\mathrm{d}t}\cdot\hat{\boldsymbol{t}}\right).\end{aligned} \tag{A 2}$$

Since

$$\frac{\mathrm{d}\hat{\boldsymbol{t}}}{\mathrm{d}t}\cdot\hat{\boldsymbol{t}}=\frac{1}{2}\frac{\mathrm{d}}{\mathrm{d}t}|\hat{\boldsymbol{t}}|^2=0, \tag{A 3}$$

we have

$$\boldsymbol{u}\cdot\frac{\mathrm{d}\hat{\boldsymbol{t}}}{\mathrm{d}t}=(\boldsymbol{u}\cdot\hat{\boldsymbol{n}})\left(\frac{\mathrm{d}\hat{\boldsymbol{t}}}{\mathrm{d}t}\cdot\hat{\boldsymbol{n}}\right). \tag{A 4}$$

The computation of $\mathrm{d}\hat{\boldsymbol{t}}/\mathrm{d}t$ proceeds as follows. Let the interface, which is a material line, be parameterized as $\boldsymbol{x}(s)$, where s is the arclength, and let the given point at time t be $\boldsymbol{x}(0)$, such that $\hat{\boldsymbol{t}} = \boldsymbol{x}'(0)$. At time $t + \Delta t$, the interface can be parameterized as

$$\boldsymbol{x}(s) + \boldsymbol{u}[\boldsymbol{x}(s)]\Delta t. \tag{A 5}$$

A tangent to this curve at the material point previously located at $\boldsymbol{x}(0)$ is found, to first order in Δt, as

$$\tilde{\hat{\boldsymbol{t}}} = \boldsymbol{x}'(0) + \boldsymbol{\nabla u} \cdot \boldsymbol{x}'(0)\Delta t = \hat{\boldsymbol{t}} + \boldsymbol{\nabla u} \cdot \hat{\boldsymbol{t}}\Delta t = \hat{\boldsymbol{t}} + \frac{\partial \boldsymbol{u}}{\partial s}\Delta t. \tag{A 6}$$

Note that $\tilde{\hat{\boldsymbol{t}}}$ may not have unit length, since s is not the arclength for the parameterization (A 5). The length N of $\tilde{\hat{\boldsymbol{t}}}$ can be expressed, to first order in Δt, as

$$N = 1 + N_1 \Delta t, \tag{A 7}$$

with $N_1 = \hat{\boldsymbol{t}} \cdot \partial \boldsymbol{u}/\partial s$. This yields, again to first order in Δt,

$$\hat{\boldsymbol{t}}(t + \Delta t) = \frac{1}{N}\tilde{\hat{\boldsymbol{t}}} = \frac{1}{1 + N_1 \Delta t}\left(\hat{\boldsymbol{t}} + \frac{\partial \boldsymbol{u}}{\partial s}\Delta t\right) = \hat{\boldsymbol{t}} + \left(\frac{\partial \boldsymbol{u}}{\partial s} - N_1 \hat{\boldsymbol{t}}\right)\Delta t, \tag{A 8}$$

such that

$$\frac{\mathrm{d}\hat{\boldsymbol{t}}}{\mathrm{d}t} = \frac{\partial \boldsymbol{u}}{\partial s} - N_1 \hat{\boldsymbol{t}} \tag{A 9}$$

and

$$\frac{\mathrm{d}\hat{\boldsymbol{t}}}{\mathrm{d}t} \cdot \hat{\boldsymbol{n}} = \frac{\partial \boldsymbol{u}}{\partial s} \cdot \hat{\boldsymbol{n}}. \tag{A 10}$$

This can be expanded further to give

$$\begin{aligned} \frac{\partial \boldsymbol{u}}{\partial s} \cdot \hat{\boldsymbol{n}} &= \frac{\partial}{\partial s}(\boldsymbol{u} \cdot \hat{\boldsymbol{n}}) - \frac{\partial \hat{\boldsymbol{n}}}{\partial s} \cdot \boldsymbol{u} = \frac{\partial}{\partial s}(\boldsymbol{u} \cdot \hat{\boldsymbol{n}}) - \left[\left(\frac{\partial \hat{\boldsymbol{n}}}{\partial s} \cdot \hat{\boldsymbol{n}}\right)\hat{\boldsymbol{n}} + \left(\frac{\partial \hat{\boldsymbol{n}}}{\partial s} \cdot \hat{\boldsymbol{t}}\right)\hat{\boldsymbol{t}}\right] \cdot \boldsymbol{u} \\ &= \frac{\partial}{\partial s}(\boldsymbol{u} \cdot \hat{\boldsymbol{n}}) - \left(\frac{\partial \hat{\boldsymbol{n}}}{\partial s} \cdot \hat{\boldsymbol{t}}\right)(\boldsymbol{u} \cdot \hat{\boldsymbol{t}}) = \frac{\partial}{\partial s}(\boldsymbol{u} \cdot \hat{\boldsymbol{n}}) - \kappa \boldsymbol{u} \cdot \hat{\boldsymbol{t}}, \end{aligned} \tag{A 11}$$

where κ is the curvature of the interface,

$$\kappa = \frac{\partial \hat{\boldsymbol{n}}}{\partial s} \cdot \hat{\boldsymbol{t}} = -\frac{\partial \hat{\boldsymbol{t}}}{\partial s} \cdot \hat{\boldsymbol{n}}. \tag{A 12}$$

Combining (A 1), (A 4), (A 10) and (A 11), we finally obtain

$$\begin{aligned} \frac{\mathrm{d}\boldsymbol{u}}{\mathrm{d}t} \cdot \hat{\boldsymbol{t}} &= \frac{\mathrm{d}}{\mathrm{d}t}(\boldsymbol{u} \cdot \hat{\boldsymbol{t}}) + (\boldsymbol{u} \cdot \hat{\boldsymbol{n}})\left[\kappa \boldsymbol{u} \cdot \hat{\boldsymbol{t}} - \frac{\partial}{\partial s}(\boldsymbol{u} \cdot \hat{\boldsymbol{n}})\right] \\ &= \frac{\mathrm{d}}{\mathrm{d}t}(\boldsymbol{u} \cdot \hat{\boldsymbol{t}}) + \kappa(\boldsymbol{u} \cdot \hat{\boldsymbol{n}})(\boldsymbol{u} \cdot \hat{\boldsymbol{t}}) - \frac{1}{2}\frac{\partial}{\partial s}(\boldsymbol{u} \cdot \hat{\boldsymbol{n}})^2. \end{aligned} \tag{A 13}$$

REFERENCES

BATCHELOR, G. K. 1967 *An Introduction to Fluid Dynamics*. Cambridge University Press.

BOZKAYA, C., KOCABIYIK, S., MIRONOVA, L. A. & GUBANOV, O. I. 2011 Streamwise oscillations of a cylinder beneath a free surface: free surface effects on vortex formation modes. *J. Comput. Appl. Maths* **235** (16), 4780–4795.

BRØNS, M. 1994 Topological fluid dynamics of interfacial flows. *Phys. Fluids* **6**, 2730–2737.

KÜCHEMANN, D. 1965 Report on the I.U.T.A.M. Symposium on concentrated vortex motions in fluids. *J. Fluid Mech.* **21**, 1–20.

LEWEKE, T., THOMPSON, M. C. & HOURIGAN, K. 2004 Vortex dynamics associated with the collision of a sphere with a wall. *Phys. Fluids* **16** (9), L74–L77.

LIGHTHILL, M. J. 1963 *Laminar Boundary Layers* (ed. L. Rosenhead), chap. 2, Oxford University Press.

LONGUET-HIGGINS, M. S. 1953 Mass transport in water waves. *Phil. Trans. R. Soc. Lond.* A **245** (903), 535–581.

LONGUET-HIGGINS, M. S. 1992 Capillary rollers and bores. *J. Fluid Mech.* **240**, 659–679.

LONGUET-HIGGINS, M. S. 1998 Vorticity and curvature at a free surface. *J. Fluid Mech.* **356**, 149–153.

LUGT, H. J. 1987 Local flow properties at a viscous free surface. *Phys. Fluids* **30** (12), 3647–3652.

LUNDGREN, T. & KOUMOUTSAKOS, P. 1999 On the generation of vorticity at a free surface. *J. Fluid Mech.* **382**, 351–366.

MALLICK, D. D. 1957 Non-uniform rotation of an infinite circular cylinder in an infinite viscous liquid. *Z. Angew. Math. Mech.* **37**, 385–392.

MORTON, B. R. 1984 The generation and decay of vorticity. *Geophys. Astrophys. Fluid Dyn.* **28**, 277–308.

OHRING, S. & LUGT, H. J. 1991 Interaction of a viscous vortex pair with a free surface. *J. Fluid Mech.* **227**, 47–70.

RAO, A., LEONTINI, J. S., THOMPSON, M. C. & HOURIGAN, K. 2013*a* Three-dimensionality in the wake of a rotating cylinder in a uniform flow. *J. Fluid Mech.* **717**, 1–29.

RAO, A., THOMPSON, M. C., LEWEKE, T. & HOURIGAN, K. 2013*b* The flow past a circular cylinder translating at different heights above a wall. *J. Fluids Struct.* **41**, 1–21.

REICHL, P. J. 2001 Flow past a cylinder close to a free surface. PhD thesis, Monash University, Melbourne, Australia.

REICHL, P., HOURIGAN, K. & THOMPSON, M. 2005 Flow past a cylinder close to a free surface. *J. Fluid Mech.* **533**, 269–296.

ROOD, E. P. 1994 Myths, math, and physics of free-surface vorticity. *Appl. Mech. Rev.* **47** (6S), S152–S156.

SARPKAYA, T. 1996 Vorticity, free surface, and surfactants. *Annu. Rev. Fluid Mech.* **28**, 83–128.

SHERIDAN, J., LIN, J.-C. & ROCKWELL, D. 1997 Flow past a cylinder close to a free surface. *J. Fluid Mech.* **330**, 1–30.

STEWARTSON, K. 1951 On the impulsive motion of a flat plate in a viscous fluid. *Q. J. Mech. Appl. Maths* **4**, 182–198.

THOMPSON, M. C., HOURIGAN, K., CHEUNG, A. & LEWEKE, T. 2006 Hydrodynamics of a particle impact on a wall. *Appl. Math. Model.* **30** (11), 1356–1369.

THOMPSON, M. C., LEWEKE, T. & HOURIGAN, K. 2007 Sphere–wall collision: vortex dynamics and stability. *J. Fluid Mech.* **575**, 121–148.

WU, J. Z. 1995 A theory of three-dimensional interfacial vorticity dynamics. *Phys. Fluids* **7** (10), 2375–2395.

WU, J. Z. & WU, J. M. 1996 Vorticity dynamics on boundaries. *Adv. Appl. Mech.* **32**, 119–275.

ZHANG, C., SHEN, L. & YUE, D. K. P. 1999 The mechanism of vortex connection at a free surface. *J. Fluid Mech.* **384**, 207–241.

View publication stats